AN ABSTRACT OF THE THESIS OF

Paul A. Crenna for the degree of Master of Science in Geology presented on December 8, 1995. Title: Late Cenozoic Tectonics of the Yubari Fold and Thrust Belt of Central Hokkaido and Implications for Opening of the Sea of Japan.

Abstract approved: Redacted for Privacy

Robert S. Yeats

Seismic-reflection, petroleum-drillhole, and surface-structure data were used to construct a balanced cross section across a Neogene fold and thrust belt on the west slope of the Yubari Mountains in Hokkaido, Japan. Syndeformational growth strata indicate at least three stages of structural development: (1) late early Miocene to middle Miocene tectonic stability, (2) middle Miocene east-west extension and normal faulting, and (3) post-middle Miocene east-west compression and reverse faulting. East-west convergence resulted in a minimum of 7 km (25%) of shortening across the Yubari Fold and Thrust Belt at a long-term-average rate of 0.8 to 1.6 mm/yr. The primary active structure is a blind reverse fault with an estimated slip rate of 0.41±0.04 mm/yr, accounting for 0.26±0.03 mm/yr of east-west convergence. An arched gravel fan, forming a fault-propagation fold in the hanging wall, corroborates late Quaternary slip on the blind fault. A dated tephra sequence providing a 110±10 ka minimum age for the fan indicates that the rate of uplift of the arch is greater than 0.66±0.17 mm/year.

The reverse faults of the Yubari Fold and Thrust Belt are reactivated middle Miocene normal faults with kilometer-scale displacements. These faults define the western margin of a graben that controlled deposition of a sequence of middle Miocene turbidites and contourites more than 4 km thick. This graben is part of an unrecognized failed crustal rift expressed as a 1000-km-long and 60-km-wide basin that contains 5-8 km of Cenozoic sediments, and includes the West Sakhalin Trough in the Russian Far East and the Ishikari-Teshiro Belt in Hokkaido. The basin exhibits many features characteristic of crustal rift zones: (1) an elevated Moho discontinuity, (2) thinned mid-crustal layers, (3) bounding normal faults and grabens, (4) thick synrift clastic sediments, and (5) association with a belt of extrusive volcanics. Hence, middle Miocene westerly extension on a crustal rift may have played an important role in the final stages of opening of the Sea of Japan.

Late Cenozoic Tectonics of the Yubari Fold and Thrust Belt of Central Hokkaido and Implications for Opening of the Sea of Japan

by

Paul A. Crenna

A THESIS

submitted to

Oregon State University

in partial fulfillment of
the requirements for the
degree of

Master of Science

Completed December 8, 1995
Commencement June 1996

Master of Science thesis of Paul A. Crenna presented on December 8, 1995

APPROVED:

Redacted for Privacy

Major Professor, representing Geology

Redacted for Privacy

Chair of Department of Geosciences

Redacted for Privacy

Dean of Graduate School

I understand that my thesis will become part of the permanent collection of Oregon State University libraries. My signature below authorizes release of my thesis to any reader upon request.

Redacted for Privacy

Paul A. Crenna, Author

ACKNOWLEDGMENT

This research was undertaken as a cooperative study between Oregon State University and the Geological Survey of Japan, and was funded by the US.-Japan Program of the National Science Foundation (NSF INT 90-144) and the Geological Survey of Japan. I thank the members of my thesis committee, Robert Yeats, Robert Lillie, Peter Clark, and Brent Dalrymple, as well as George Moore for reviewing my manuscript. I also thank Y. Kinugasa and all the members of the Seismotectonics Section of the Survey for their hospitality, discussions about the geology of Japan, and logistical support. I am especially grateful to K. Okumura, E. Tsukuda, and K. Shimokawa, who collected, analyzed and interpreted Quaternary data for this project. I also thank the Japan Petroleum Exploration Company, Ltd. (JAPEX), which kindly provided unpublished field maps, well logs, cross sections, biostratigraphic data, and seismic-reflection records. I personally thank geologists T. Kodato and M. Kuniyasu for their efforts in retrieving and explaining the JAPEX data. In addition, I thank K. Kanagawa and the employees of the Haiji Bokujo Ranch in Hokkaido, who provided base-camp facilities and made me feel at home in a foreign country.

TABLE OF CONTENTS

TABLE OF CONTENTS , Continued

LIST OF FIGURES

LIST OF FIGURES, Continued

LIST OF FIGURES IN APPENDICES

LATE CENOZOIC TECTONICS OF THE YUBARI FOLD AND THRUST BELT OF CENTRAL HOKKAIDO AND IMPLICATIONS FOR OPENING OF THE SEA OF JAPAN

INTRODUCTION

This study investigates the structure and tectonics of the Yubari Fold and Thrust Belt on the west flank of the Yubari Mountains in Hokkaido, Japan (Figure 1). The Yubari Fold and Thrust Belt (onshore) is a 30-km-wide, 140-km-long band of Neogene marine sedimentary rocks characterized by westward-vergent, tight to isoclinal folds and faults indicative of east-west contraction (Kimura et al., 1983; Geological Survey of Japan, 1992). This fold and thrust belt forms the foreland of a larger zone of intracontinental convergence located between the northeast Japan volcanic arc and the Kuril volcanic arc, which includes the Ishikari Lowland, the Yubari Mountains, and the Hidaka Mountains (Kimura, 1986; Okumura, 1987; Figure 2). The root structure of the convergence zone is a 60°-east-dipping, crustal megathrust, seismically imaged beneath the Hidaka Mountains, which reactivated a Mesozoic suture and exhumed metamorphosed lower crust, including radiometrically-dated granitic intrusions as young as 17 Ma (Shibata et al., 1984; Miyamachi and Moriya, 1984; Jolivet and Huchon, 1989).

Paleostress-field data from Hokkaido indicate that east-west convergence began in the late Miocene and has continued to the present (Kimura, 1981, 1986; Yamagishi and Watanabe, 1986; Okumura, 1987). On the west, the fold and thrust belt borders a sub-basin of broadly folded Quaternary and late

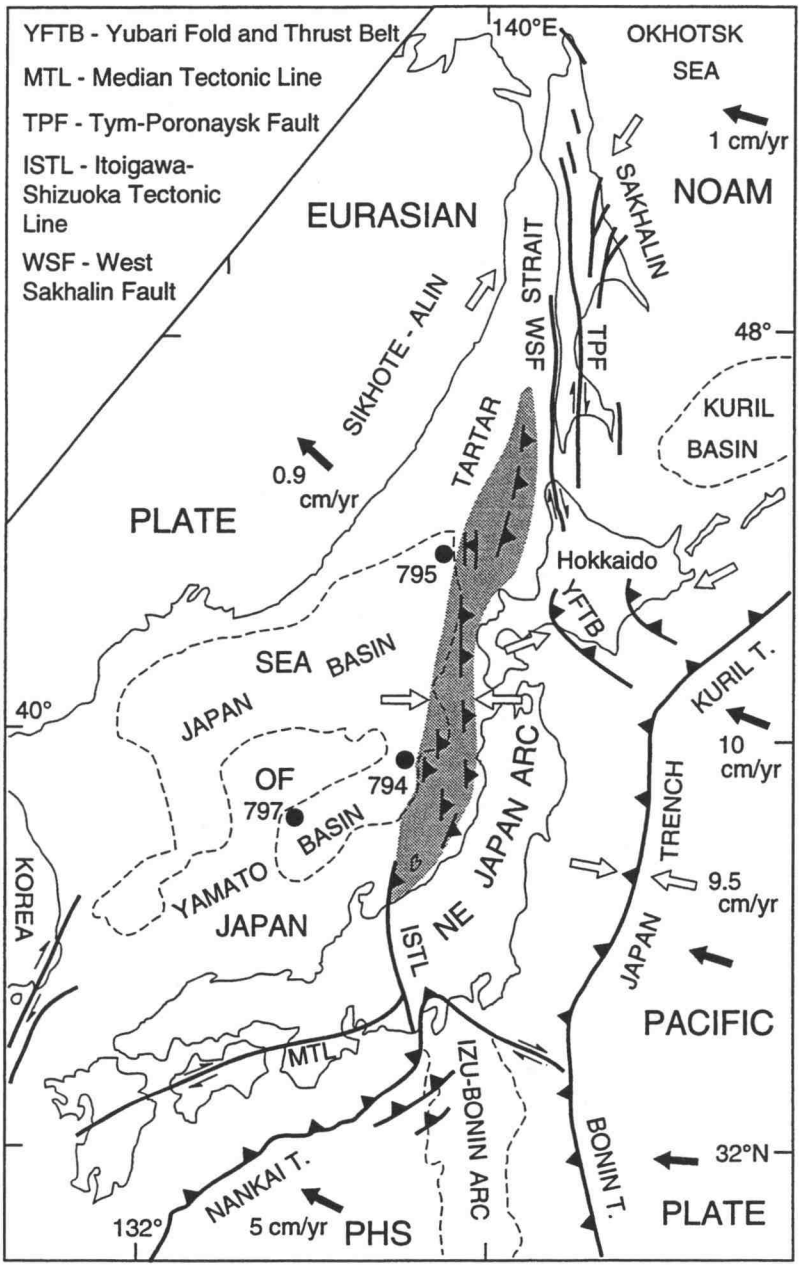

Figure 1 Geodynamic setting of Japan and Sakhalin modified from Nakamura (1983), Seno (1985), Okumura (1987), Fournier et al. (1994), and Moore et al. (1994). Solid arrows denote absolute motion relative to fixed hotspots under Pacific Plate after DeMets et al. (1990). Open arrows indicate relative plate motion. Zone of recent compression is shaded. PHS - Philippine Sea Plate, NOAM - North American Plate.

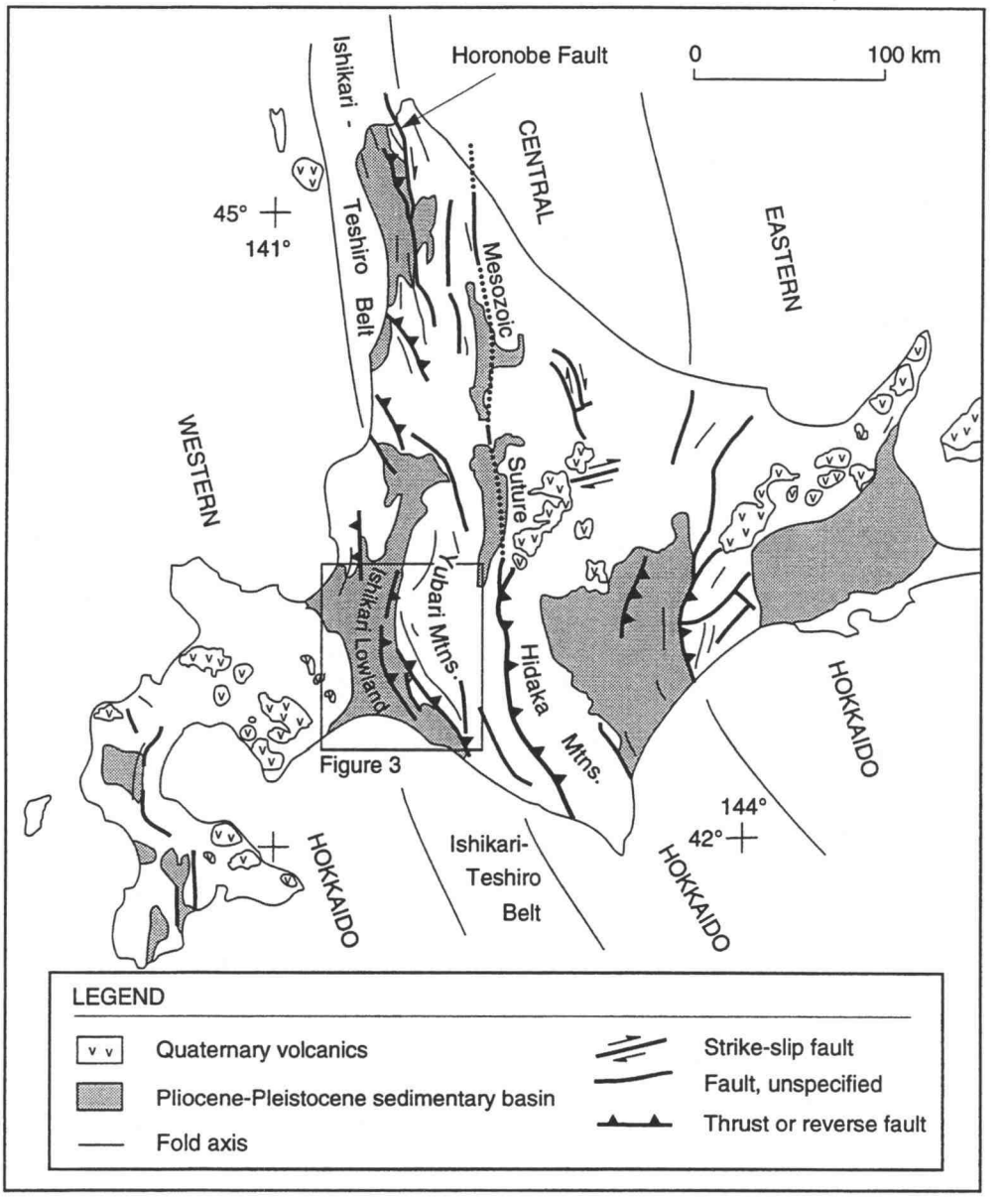

Figure 2 Neotectonic map of Hokkaido. Interarc convergence zone between the northeast Japan and Kuril volcanic arcs includes the Ishikari Lowland foreland basin, the Yubari Fold and Thrust Belt on the west slope of the Yubari Mountains, and a crustal megathrust in the Hidaka Mountains that reactivated a Mesozoic suture. En echelon volcanic ridges projecting into thrust faults may mask oblique strike-slip faults accommodating westward translation of the Kuril forearc.

Pliocene marine sediment underlying the Ishikari Lowland (Figure 3). Tilted marine terraces and late Quaternary fault scarplets indicate that active structures control the boundary between the Ishikari Lowland and the Yubari Fold and Thrust Belt, but because the primary faults are blind, the rate of activity is poorly constrained (Research Group for Active Faults in Japan, 1991).

During the Paleogene and early to middle Miocene, the Sea of Japan opened as a pull-apart basin between two dextral shear zones, one located east of Korea and the other in central Hokkaido and Sakhalin, Russia (Lallemand and Jolivet, 1986) (see Figure 1). Strike-slip faulting triggered southerly extensional rifting and seafloor spreading in the incipient Sea of Japan that was accompanied by widespread volcanism from 28-18 Ma (Tamaki et al., 1992). Pervasively deformed Paleogene and early Miocene rocks define a broad, 1000-km-long dextral strike-slip shear zone in central Hokkaido and Sakhalin, which marked the Tertiary boundary between the Eurasian and North American Plates (Kimura et al., 1983; Kimura and Tamaki, 1986; Lallemand and Jolivet, 1986; Jolivet and Huchon, 1989; Fournier et al., 1994).

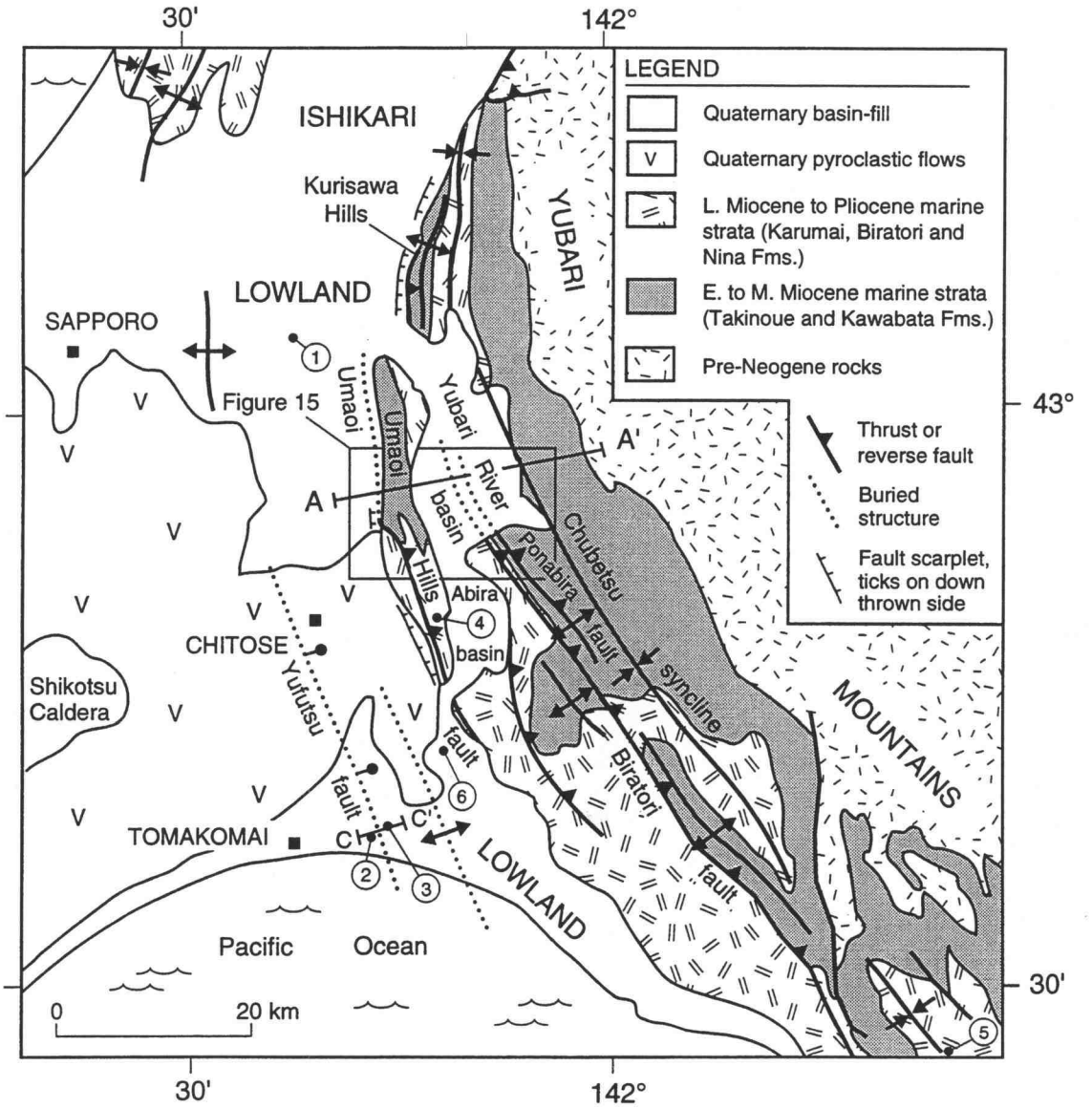

Figure 3 Neotectonic map of the Yubari Fold and Thrust Belt and Ishikari Lowland (modified from Sangawa et al., 1984). Petroleum industry drillholes: 1 Miti Nanporo, 2 Minami Yufutsu SK-2D, 3 Yufutsu SK-1, 4 Abira SK-1, 5 Niikappu SK-1, and 6 drillhole from Kondo et al. (1984).

GEODYNAMIC SETTING

Oceanic crust of the Pacific Plate is subducting westward at a rate of 10 cm/year beneath continental crust of the northeast Japan and Kuril volcanic arcs (DeMets et al., 1990; Moore et al., 1992)(Figure 1). In the past few decades, several major thrust-type earthquakes (>M7) have occurred in the eastern Sea of Japan, indicating that oceanic crust in the Sea of Japan is also thrusting beneath the northeast Japan arc (Nakamura, 1983). This zone of "nascent subduction" may connect with the Itoigawa-Shizuoka Tectonic Line to form the intracontinental plate boundary between Eurasia and North America, such that northeast Japan is coupled with the North American Plate (Nakamura, 1983; Seno, 1985). North of Hokkaido, in Sakhalin, Russia, seismically active thrust and strike-slip faults indicate that the intracontinental boundary there is transpressional (Chapman and Solomon, 1976; Fournier et al., 1994), while young, northwest-striking, en echelon fold axes and thrust faults in the Ishikari-Teshiro Belt suggest that this transpressional stress regime also extends into northern Hokkaido (Kimura et al., 1983).

Two driving mechanisms for interarc convergence in south-central Hokkaido have been proposed. The first hypothesis is that the convergence zone was the primary boundary between the North American and Eurasian Plates from the Miocene to the Pleistocene, but that this boundary has now shifted to the nascent subduction zone in the eastern Japan Sea (Chapman and Solomon, 1976; Seno, 1985; Research Group for Active faults in Japan, 1991). The second hypothesis proposes that convergence is driven by oblique subduction of the Pacific Plate beneath the Kuril arc (Kimura et al., 1983;

Kimura, 1986). Slip vectors for thrust earthquakes are slightly oblique (1-12°) and predict arc-parallel contractional strain on the subduction boundary of 17.8±18.8 mm/yr at the cusp between the Kuril and northeast Japan arcs (McCaffrey, *in press*). According to the second hypothesis, westward translation of the Kuril forearc is accommodated by mid-arc dextral shear on discontinuous strike-slip faults and P-shears, interpreted to control the remarkable en echelon arrangement of Quaternary volcanoes in and around Hokkaido (Figure 2). Deformation of a widespread, last interglacial (0.13 Ma) marine terrace documents thrust faulting and eastward tilting of crustal blocks in southern Hokkaido, consistent with the forearc-migration hypothesis (Okumura, 1987).

DATA AND METHODS

Structural data were incorporated from seismic-reflection records, petroleum drillholes, and surface mapping. Three overlapping seismic-reflection lines provide 21 kilometers of continuous east-west coverage. Two are unmigrated industry records (Yuni-Shuhen V6 and V7) collected during a 1977 Vibroseis survey with a shot-point interval of 25 m. Time to depth conversion of these records was accomplished using a modified version of the depth-conversion chart of Asano et al. (1985) and is discussed in Appendix 1. Migration of the records was performed by hand using techniques described in Lindseth (1968). The third record (Naganuma 85) is of lower resolution (shot-point interval of 50 m), but includes migrated-time and migrated-depth records (Asano et al., 1985).

Logs of petroleum industry drillholes in and around the central Umaoi Hills show lithology, dipmeter readings, dips from drillcores, and biostratigraphic zones. Less detailed drillhole data were taken from previous studies (Agatsuma, 1961, 1962; Tsuchida, 1961; Mitani, 1978) and summary reports compiled by universities and government offices (Commission for the Promotion of Mining in Hokkaido, 1968; Niitsuma et al., 1982; Commission for the Promotion of Mining in Hokkaido, 1990; Okamura et al., 1992). Surface structural data from published geologic maps were supplemented by industry field maps and data from 280 field exposures in a 140 km^2 area of the central Umaoi Hills. Data collected by the Geological Survey of Japan include a 1.8-km-long, high-resolution, seismic-reflection record and two drillcores, 50 and 180-m long.

STRATIGRAPHY

The Neogene stratigraphy of the Yubari Mountains and Ishikari Lowland is known from work by the petroleum industry and 1:50,000-scale mapping by the Geological Survey of Japan (Maiya et al., 1981). From the early Miocene to the Pleistocene, this region was a marine basin receiving more than 4 km of conformable sediments (Maiya, 1981; Okada, 1983; Hoyanagi et al., 1986), that were capped by late Quaternary terrestrial gravel and coastal estuary deposits. Paleogene marine strata underlie the Neogene section unconformably and are encountered in four drillholes in the Ishikari Lowland: Nishi-Umaoi SK-3, Miti-Nanporo, Abira SK-1, and Minami Yufutsu SK-2D (see Figure 3). The Paleogene, in turn, rests unconformably on Cretaceous ophiolite, encountered in Miti-Nanporo and Minami Yufutsu SK-1.

Neogene Biostratigraphy

A detailed Tertiary biostratigraphy based on the vertical distribution of fossils, including more than 236 species of foraminifers (mostly benthic), and 165 species of mollusks, diatoms, and other fossils, was developed by the petroleum industry (Agatsuma, 1962; Figure 4). Although benthic foraminiferal zones may be more reflective of water depth than time (Ponti et al., 1993), the biostratigraphic zones in the Ishikari region are considered good approximations of time-stratigraphic units, and have been formally correlated with the planktonic chronostratigraphic scheme devised by Blow (1969), based on drillcore biostratigraphy from the Deep Sea Drilling Project (Maiya et al., 1981). All of the Neogene numerical ages cited in this study are based on these

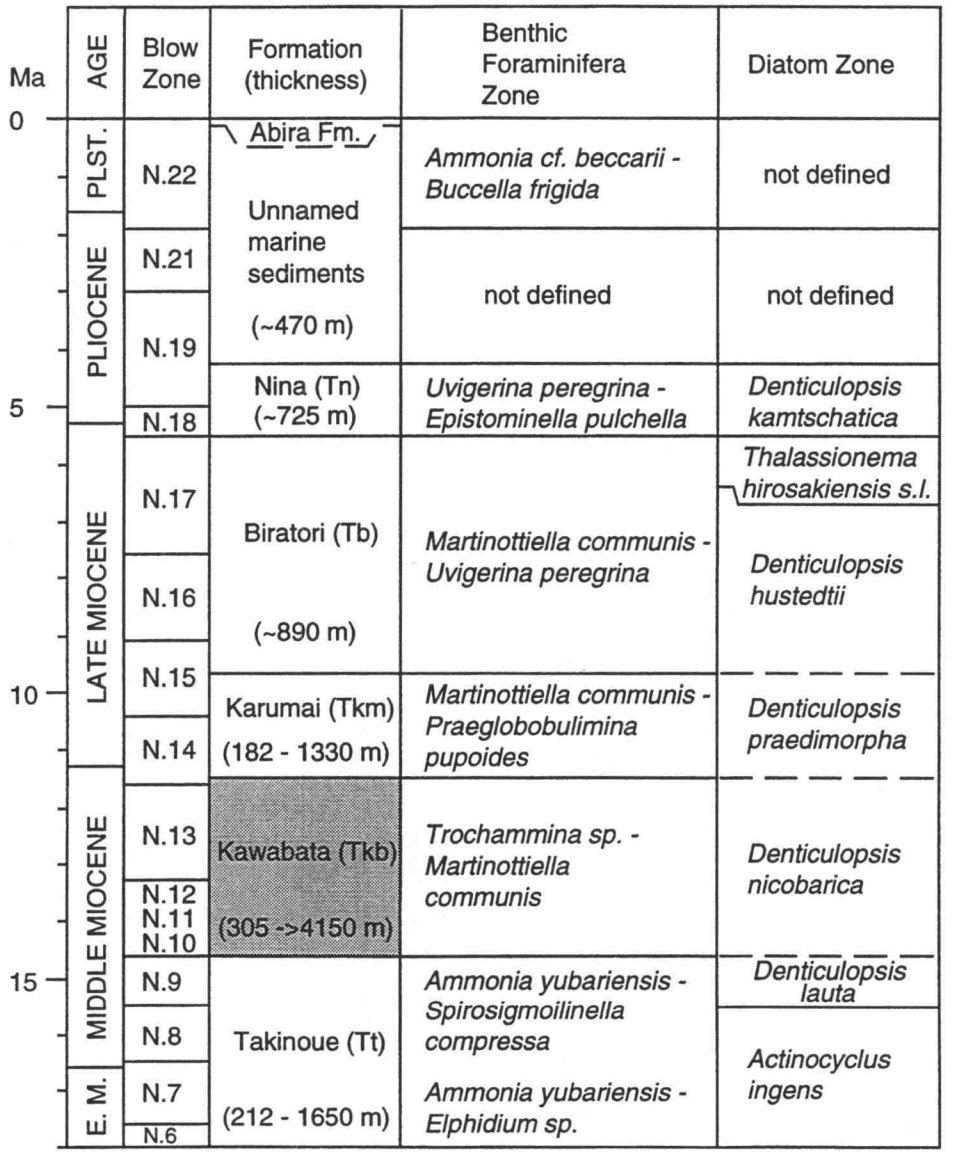

Figure 4 Biostratigraphic and chronostratigraphic correlation of late Cenozoic formations in the Ishikari area after Maiya et al. (1981). Approximate boundaries between biozones are dashed. Quaternary section modified from Umaoi Collaborative Research Group (1987).

time-stratigraphic units. The age of the Takinoue Formation, the lowermost unit of the section, is the best constrained, because it contains molluscan fauna unique to a widespread, warm-water species assemblage found only within planktonic foraminiferal zones N.8 and N.9 (Chinzei, 1986).

Neogene and Quaternary Lithostratigraphy

A 2,400-m-thick composite stratigraphic section, compiled from surface exposures in the central Umaoi Hills, was modified from Agatsuma (1961) and used for subsurface correlation. The Takinoue Formation consists of very-fine- to coarse-grained siltstone with minor interbeds and lenses of fine sandstone (<5%), tuffaceous sandstone, and tuff. The Kawabata Formation consists of fine- to medium-grained sandstone (85%) with interbeds of siltstone, tuff, and sills of basaltic andesite and volcanic breccia up to 100 m thick. The Karumai Formation consists of hard shale interfingering with mudstone, particularly in the upper 50 m, and is commonly interbedded with sandstone in the middle section. The Biratori Formation consists of sandy siltstone (95%) with minor interbeds of fine-grained sandstone and conglomeratic sandstone. The Nina Formation is informally divided into a lower member consisting of siltstone, encountered in Nishi Umaoi SK-1, and an upper member, consisting of conglomerate and sandstone turbidites with "rip-up" blocks of siltstone up to 50 m in diameter. Unnamed Pliocene and Quaternary marine sediment overlies the Nina Formation in the Ishikari Lowland and are described in the Nishi Umaoi SK-1 well log as 310 m of siltstone overlain by 160 m of sandy gravel.

Late Pleistocene Terrestrial Gravel (Abira Formation)

The surficial geology of the Abira and Yubari River basins east of the Umaoi Hills is dominated by a widespread, late Pleistocene gravel deposit greater than 25 m thick (Umaoi Collaborative Research Group, 1987). In the central Umaoi Hills and Yubari River basin, the deposit consists of 1-meter-thick beds of poorly-sorted, sandy gravel (50%-80%) containing lenses of silt and laminated sand with stringers of fine pebbles. Most of the gravel beds are composed of subrounded to rounded fine pebbles to cobbles (20 cm maximum diameter) in a matrix of fine- to coarse-grained sand, and exhibit a massive, graded, or weakly imbricated structure.

The age of the gravel is not known directly; but, fission-track dates of late Pleistocene tephras overlying the gravels limit the age of abandonment of the gravel fan to before 110±10 ka (Machida et al., 1987; Okumura, 1988; Figure 5). The lower age constraint is provided by a magnetic-polarity log of correlative sediment in the Abira River drainage to the south (Kondo et al., 1984). In this drillcore, correlative gravel lies within a normal polarity interval that includes the late Pleistocene tephra sequence (Figure 5). Hence, this gravel is younger than the 0.78 Ma base of the Brunhes geomagnetic chron (Hilgen, 1991).

Late Pleistocene Tephra

A series of widespread tephras (>50,000 km^2) from explosive volcanic eruptions in Japan and Korea blanketed the late Quaternary landscape of northern Japan (Arai et al., 1986; Okumura, 1991: Figure 5). The refractive

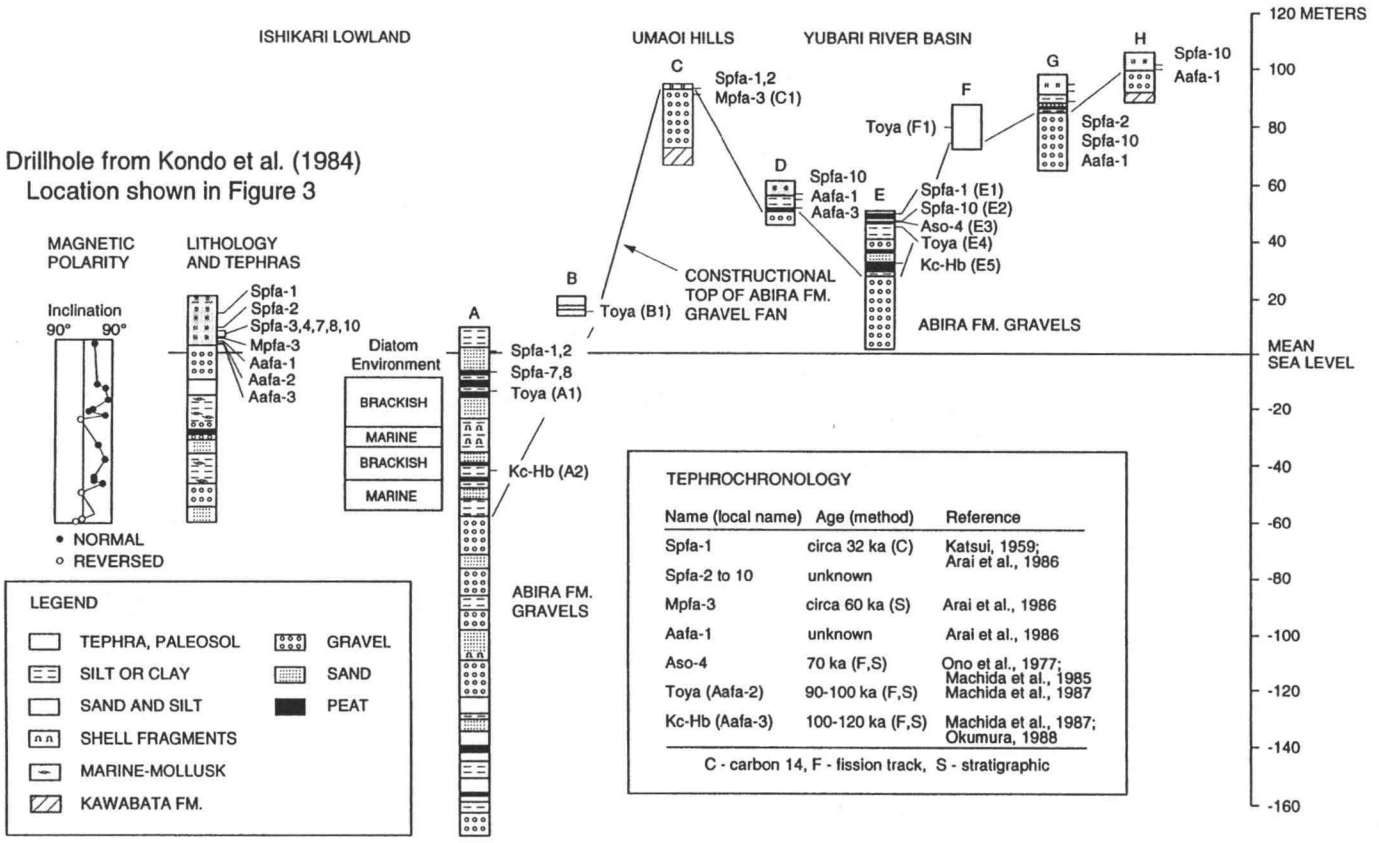

Figure 5 Correlation of columnar sections from exposures and drillcores in the Abira Formation. Columns A,C,E, and F are unpublished data from the Geological Survey of Japan. Columns D, G, and H are taken from Umaoi Collaborative Research Group (1987), and column B is from Okumura (1987). Tick marks are tephras identified from their mineralogy, major-element chemistry, and refractive index. Locations of columnar sections are shown in Figure 15.

index, major-element geochemistry, and mineralogy of these tephras have proven to be an accurate means of correlation (Arai et al., 1986). Ages of the more widespread tephras have been determined primarily by the fission-track method on zircon or obsidian fragments and radiocarbon dating (Arai et al., 1986; Machida et al., 1987). Tephras from two drillcores (A and E) and several surface exposures (B and F) were identified by K. Shimokawa of the Geological Survey of Japan based on major-element chemistry and refractive index (Figure 5). Analytical procedures and results are summarized in Appendix 2.

STRUCTURE OF THE YUBARI FOLD AND THRUST BELT

The Umaoi Hills expose a 5-km-wide, 40-km-long zone of complexly deformed Neogene strata (Agatsuma, 1961; Ishida et al., 1980) in the frontal region of the Yubari Fold and Thrust Belt (Figure 3). New field mapping in a 140 km^2 part of the central Umaoi Hills (Figure 6) combined with subsurface data enabled construction of a balanced cross section across the fold and thrust belt (Figure 7). Folds are projected into the subsurface using the kink-band method of Suppe (1985) and Boyer (1986), which allows calculation of shortening.

Northern Umaoi Anticline

The northern Umaoi anticline is a 15-km-long and 4-km-wide, asymmetrical fold associated with the east-dipping Umaoi reverse fault (Figure 7). The forelimb, adjacent to the fault, consists of steeply dipping to overturned strata cut by secondary faults, and the backlimb consists of strata inclined 40° to 60°E. The axis of the anticline is offset by an axis-parallel fault (Ishida et al., 1980), termed a high-angle breakthrough fault by Suppe (1990). Exposures of the fault show a dip of 44° E and limit reverse separation of the Takinoue-Kawabata contact to less than a few hundred meters (see Figure 6). In Figure 7, the high-angle breakthrough fault is inferred based on the absence of west-dipping beds of Takinoue in the core of the anticline. Area balancing indicates a minimum of about 350 m of reverse separation.

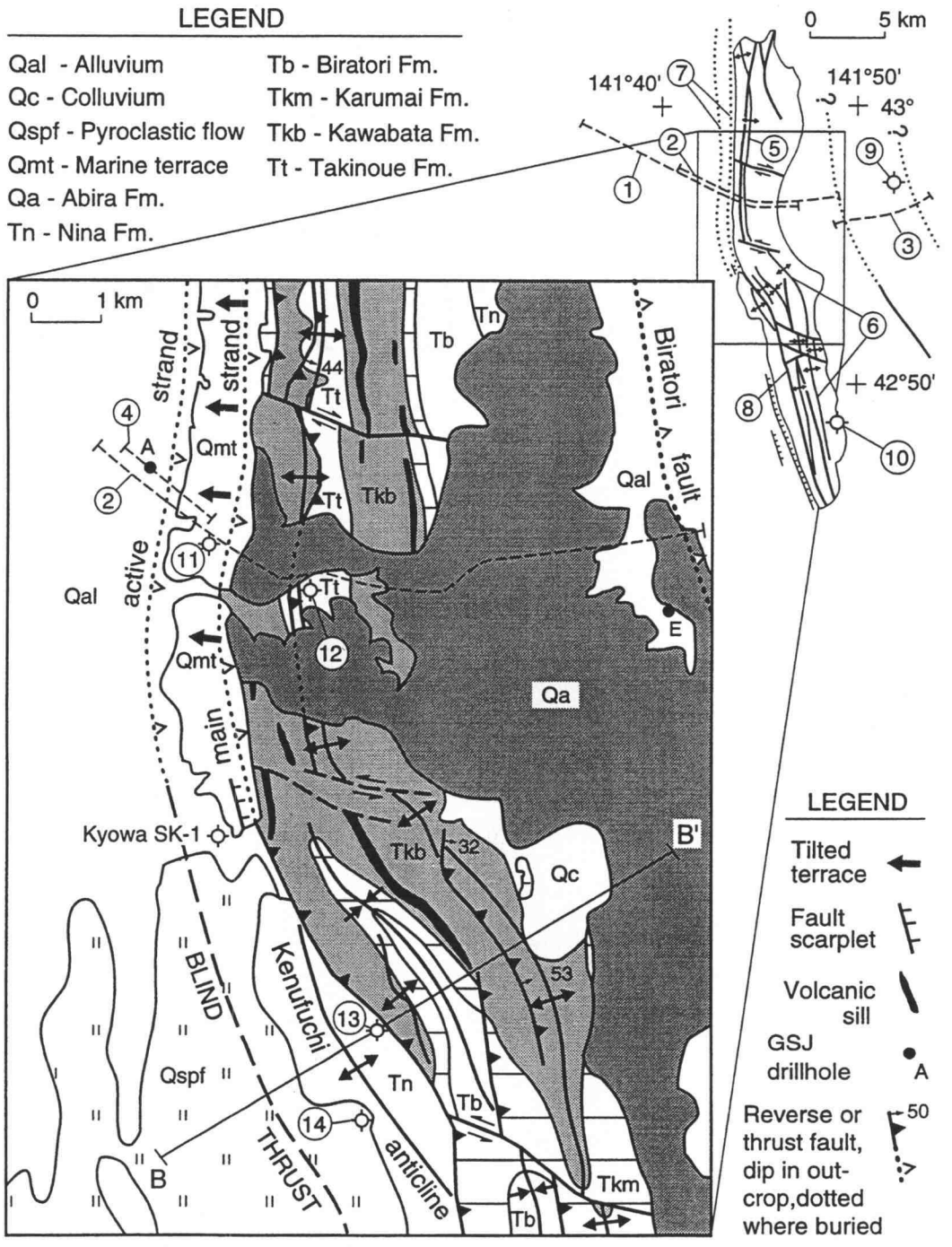

Figure 6 Simplified geologic map of the central Umaoi Hills. Seismic-reflection lines: (1) Naganuma 85, (2) Yuni-Shuhen V6, (3) Yuni-Shuhen V7, (4) high resolution line. Structures: (5) Northern Umaoi Anticline, (6) Southern Umaoi Anticline, (7) northern segment Umaoi Fault zone, (8) southern segment Umaoi Fault. Petroleum drillholes: (9) Yuni SK-1, (10) Abira SK-1, (11) Nishi-Umaoi SK-1, (12) Umaoi-Yama R-1, (13) Nishi-Umaoi SK-2, (14) Nishi Umaoi SK-3.

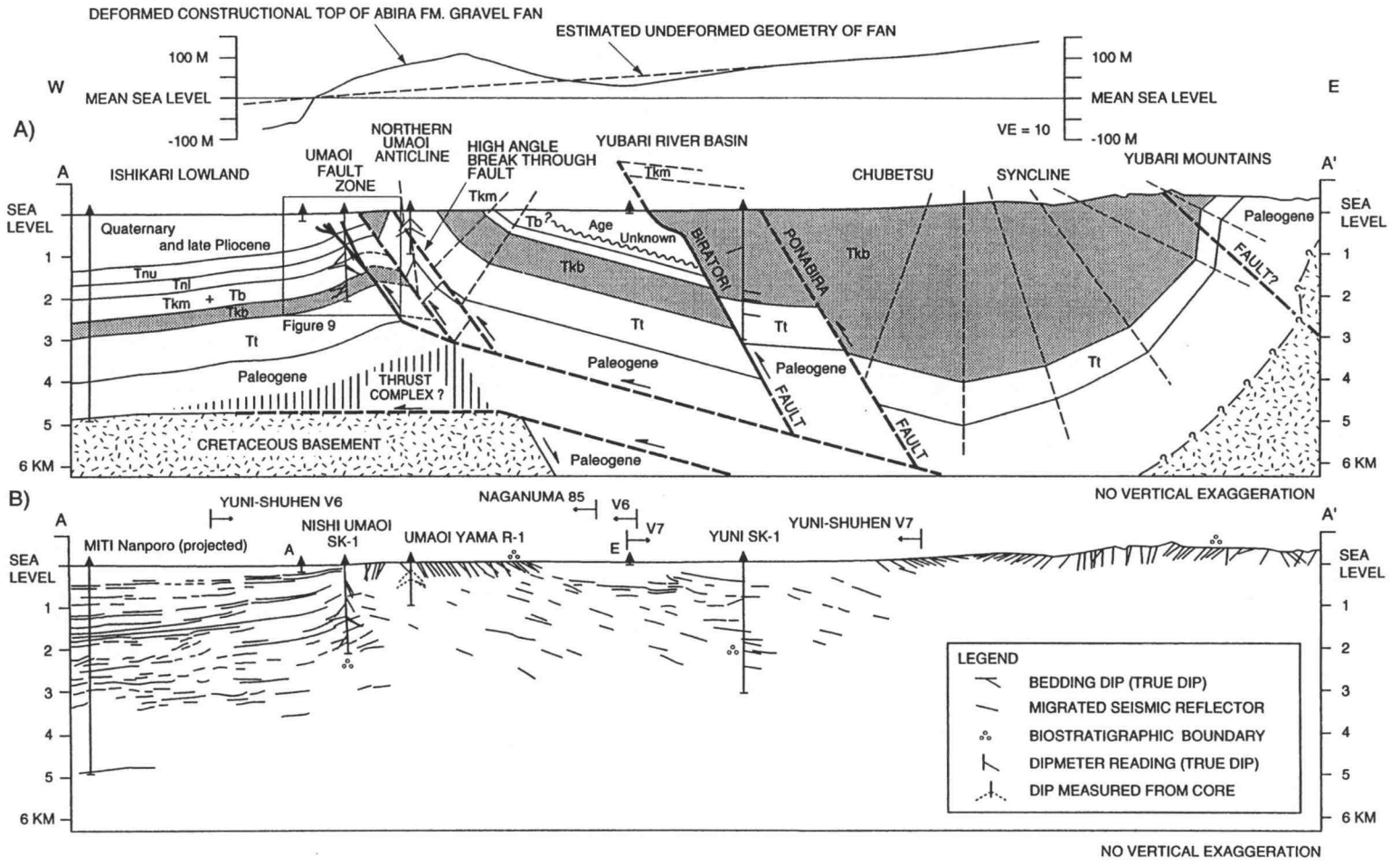

Figure 7 (a) Balanced structure section across of the Yubari Fold and Thrust Belt. Profile above section shows deformed and undeformed constructional top of the Abira Formation gravel fan. Note that profile follows nose of fan, as shown in Figure 15, and; therefore, differs somewhat from the line of section. (b) Primary data set used to construct the structure section. Location of section is shown in Figure 3.

Umaoi Fault

The Umaoi Fault is a 45-km-long reverse fault that extends along the western rangefront of the Umaoi Hills (Agatsuma, 1961; Tsuchida, 1961). This study divides the fault into a northern segment controling the rangefront of the northern Umaoi Hills, and a southern segment lying within the southern Umaoi Hills (Figure 6).

Northern Segment

The northern segment of the Umaoi Fault is buried beneath late Pleistocene deposits, but is constrained to a 700-m-wide zone between the Nishi Umaoi SK-1 well and surface exposures (Figure 6). On seismic-reflection profile Yuni-Shuhen V6, strong, continuous reflectors in the footwall warp up into the fault zone and show that the fault dips to the east (Figure 8). These west-dipping reflectors terminate along an east-dipping plane which projects to the near-surface location of the fault and is interpreted to be the main strand of the fault. Correlation of seismic reflectors with biozones in Nishi Umaoi SK-1 indicates that the fault juxtaposes Pliocene and Quaternary strata in the footwall with Kawabata Formation exposed in the western Umaoi Hills (Figure 8). Reverse separation of the top of the Kawabata is about 1,750 m (Figure 7). Four dipmeter readings of 60°-67°E and two drillcore dips of 50° and 52° in the log of Nishi Umaoi SK-1, west of the main strand, suggest the fault dips 50-70° E (Figure 9).

Another strand of the fault, a curved surface dipping to the east, lies about 1 km west of the main strand and is delineated by a break in reflector continuity below 0.5 seconds and sharply upwarped reflectors above 0.5

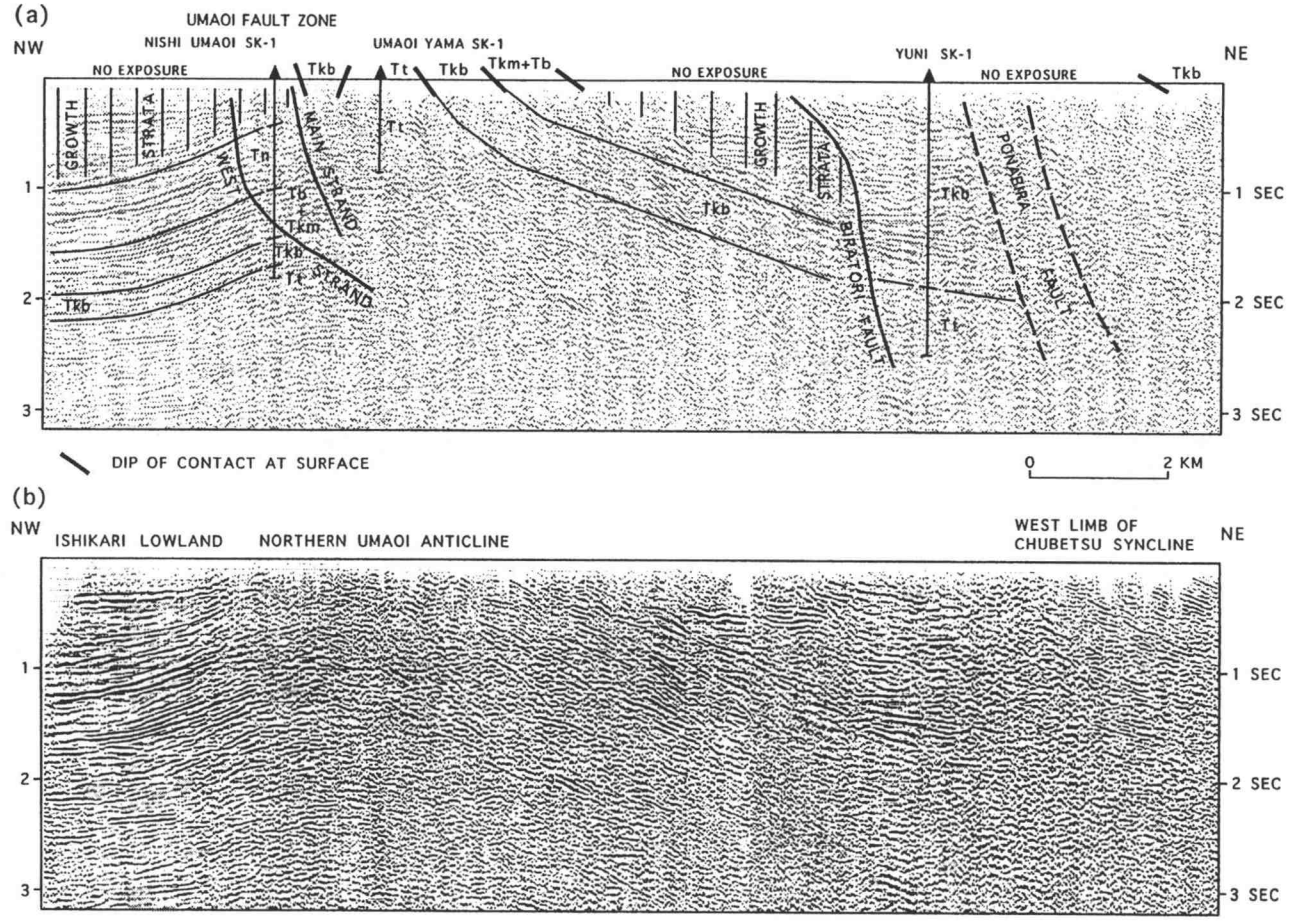

Figure 8 (a) Interpretation of unmigrated seismic-reflection records Yuni-Shuhen V6 and V7 showing structures, reflector correlations with wells and surface exposures, and growth strata. (b) Unmigrated seismic-reflection records Yuni-Shuhen V6 and V7. Locations shown in Figure 6.

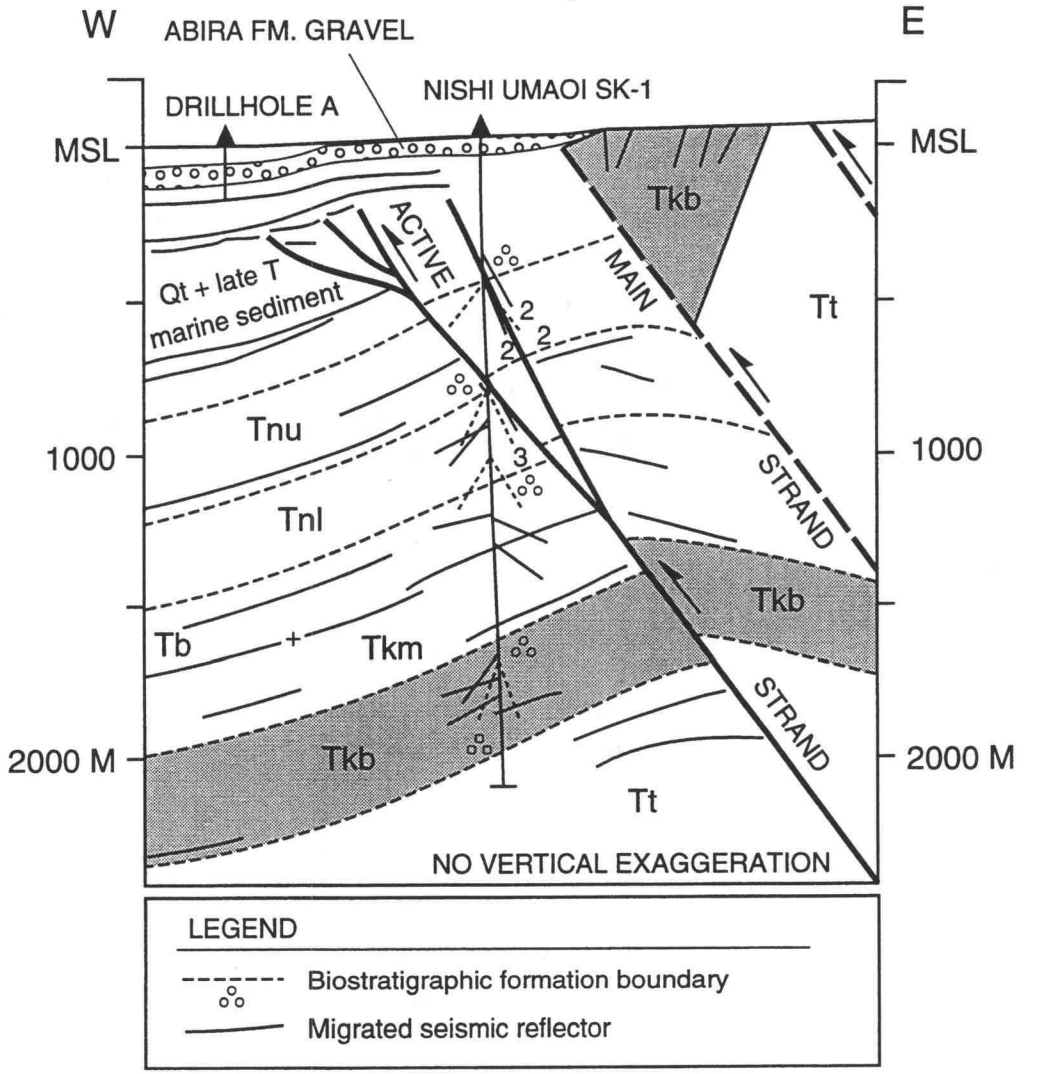

Figure 9 Detailed structure of the northern segment of the Umaoi Fault. Location shown as inset in Figure 7.

seconds (Figure 8). This fault plane appears listric on the unmigrated time section, but defines a subplanar surface dipping 50°E after migration and depth conversion (Figure 9). Where the Nishi Umaoi SK-1 drillhole crosses the fault, the dipmeter log shows a dip of 60° E and the drillcore log shows three dips of about 65°. The apparent lack of repeated strata in the well log limits the amount of vertical displacement on the westernmost strand to less than a few hundred meters.

Southern Segment

The southern segment of the Umaoi Fault offsets Pliocene Nina Formation at the surface and is associated with active fault scarplets subparalleling the fault trace a few kilometers to the west (Figure 6). The dip of the southern segment is not known, but subsurface data suggest the fault branches from a major blind thrust underlying the Umaoi Hills (Figure 10). In Abira SK-1, this thrust brings Paleogene rocks over Takinoue at a depth of 4 km. Missing sections in Nishi Umaoi SK-2 and Kyowa SK-1 may be explained as a projection of the blind thrust parallel to bedding from Abira SK-1. Nearer to the surface, this projection coincides with a fold hinge in the west limb of the Kenufuchi Anticline. The sharp change in dip from 60° to 80° in Pliocene strata compared to 8° to 38° in underlying strata may be interpreted as the forelimb of a fault-propagation fold (Suppe and Medwedeff, 1990) which is absorbing slip on the blind thrust. East-facing fault scarplets are found exclusively within this zone of young, steeply-dipping strata at the rangefront (Research Group for Active Faults of Japan, 1991) suggesting that they are bedding-parallel, flexural-slip faults related to active folding above the tip of a blind thrust.

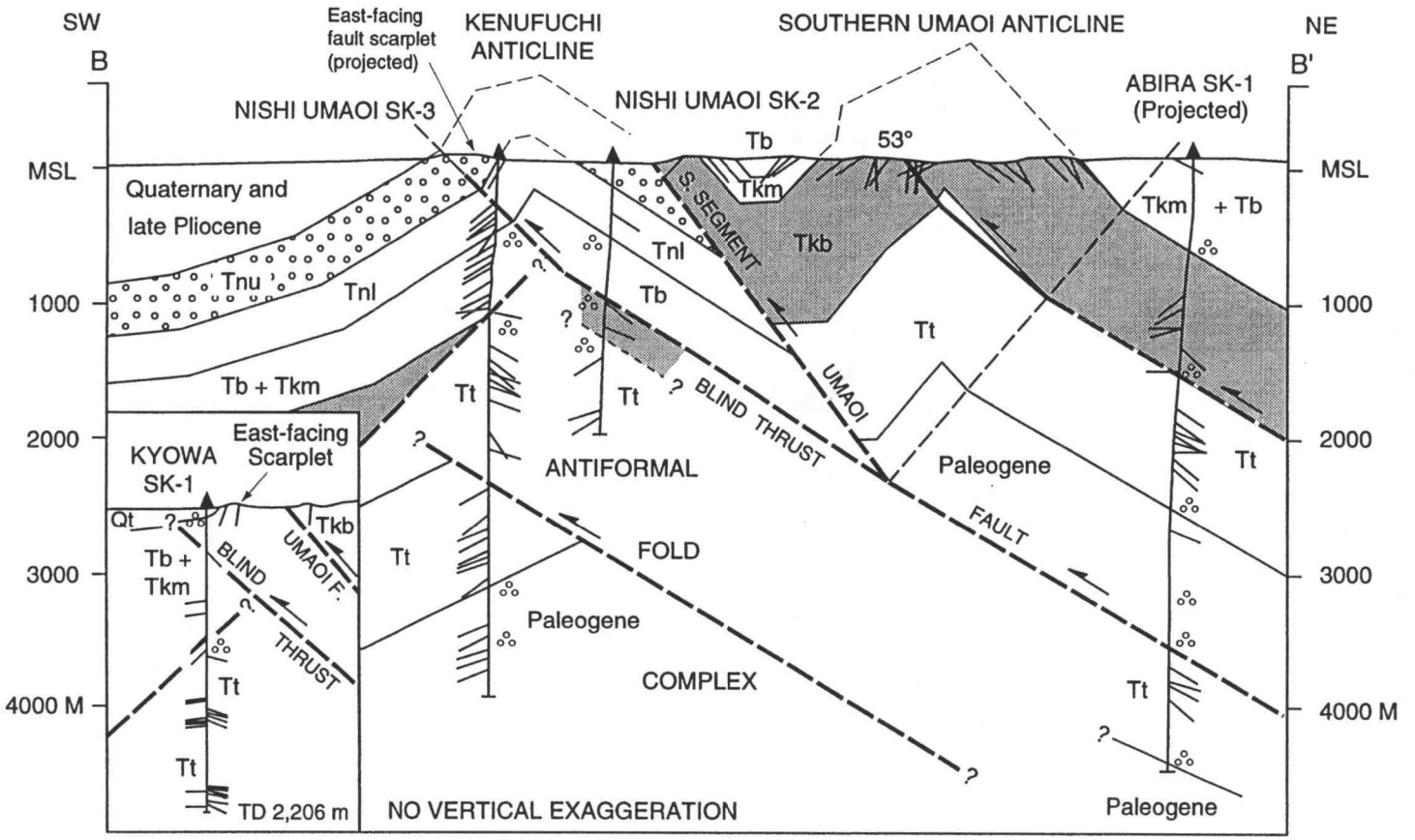

Figure 10 Structure section of the south-central Umaoi Hills based on drillhole and surface data. Fault slip on blind strand of the Umaoi Fault is taken up in fault-propagation folding of the Kenufuchi anticline. East-facing fault scarplets above steeply dipping Pliocene strata indicate flexural slip on bedding planes associated with late Quaternary activity on blind thrust. Line of section is shown in Figure 6. Inset shows additional structure data from a nearby well, Kyowa SK-1.

Biratori Fault

The surface trace of the Biratori Fault is 60 km long and strikes 325° (see Figure 3). The northern end of the fault projects beneath late Quaternary sediment and intersects seismic-reflection record Yuni-Shuhen V7, where it is expressed as an east-dipping structural boundary between three groups of uniformly dipping reflectors (Figure 8). The structure on the west side of the fault is defined by a group of inclined reflectors (15°E) correlated with strata exposed on the east slope of the Umaoi Hills. East of the fault, the structure is defined by a group of gently dipping reflectors (2°E) and dipmeter data from Yuni SK-1 (Figure 7). After migration and depth conversion, these reflectors confine the orientation of the fault plane to about 60°E at depth, about 30°E near the surface.

Correlation of seismic reflectors with drillcore and outcrop biostratigraphy indicates that the Biratori Fault juxtaposes Karumai and Biratori Formations in the footwall against the Kawabata Formation in the hanging wall (Figure 7). Reverse displacement of the upper contact of the Kawabata is greater than 2,600 m. Erosion has removed most of the overlying Karumai Formation from the hanging-wall block; however, remnants preserved to the south indicate that the Karumai was once continuous across the fault (Matsuno and Ishida, 1960; Ishida et al., 1980) (see Figure 3). A down-plunge structural projection, shown in Figure 7, indicates that the true stratigraphic thickness of the Kawabata Formation in the hanging wall is about 2,700 m, and that the total reverse separation of the top of the Kawabata is about 3,250 m.

Ponabira Fault

East of the Biratori Fault, a vertical zone of low reflectance separates 15° east-dipping reflectors on the western limb of the Chubetsu Syncline from 2° east-dipping reflectors (Figure 8). This zone lies on the northwestern projection of an unnamed fault associated with the Ponabira anticline that has a map trace 10 km long (Matsuno and Hata, 1960; Matsuno and Ishida, 1960; Ishida et al., 1980) (Figure 3). This fault coincides with a thickness change in the Kawabata Formation from about 2,700 m at Yuni SK-1 to greater than 4,150 m in the Chubetsu Syncline (Figure 7).

Chubetsu Syncline

The Chubetsu Syncline is a 13-km-wide, 50-km-long fold bounded on the east by upwarped Paleogene and Cretaceous rocks in the Yubari Range and on the west by the Biratori Fault (Sangawa et al., 1984; Figure 3). The structure of the syncline is constrained by many bedding attitudes and east-dipping reflectors on the Yuni-Shuhen V7 profile (Figure 7). No wells within the syncline have penetrated the Kawabata Formation, but one well (Niikappu SK-1) on the south-central coast of Hokkaido penetrated a 3,075 m thickness of Kawabata without reaching its base (see Figure 3). The thickness of the Kawabata Formation shown in figure 7 is a minimum estimate based on projection of surface data and is consistent with previous estimates by Matsuno and Ishida (1960), Agatsuma (1961), and Mitani (1978).

TECTONIC EVOLUTION

The geometry, thickness, and age of sediment deposited during deformation provides evidence for structural growth. Such sediment is termed "growth-strata" (Suppe et al., 1992). The Neogene strata of the Yubari Fold and Thrust Belt were deposited during deformation, and record at least three stages of structural development (Figure 11). These stages were used as a framework for retrodeformation and balancing of structure section A-A'. The direction of tectonic transport is estimated to be 260°, based on pervasive westward vergence and the westward-convex shape of the deformation front.

Late Early to Middle Miocene (Stage 1)

The Takinoue Formation is inferred to predate dip-slip faulting based on its gently northeast-tapering geometry (Figure 11). Isopachs show that the Takinoue thins gradually to the northeast from 1,650 m at the Minami Yufutsu SK-2D well in the Ishikari Lowland to 250 m in the Yubari Mountains (Figure 12). This gentle wedge geometry is largely due to southwestward-thickening beds of volcanic ash. Submarine erosion of tectonic growth features seems unlikely given the consistent silt grain size of the Takinoue Formation and the conformable nature of its upper contact (Maiya et al., 1981). Hence, from 18 to 14 Ma, tectonic growth of local structures did not significantly affect sediments in the Takinoue basin.

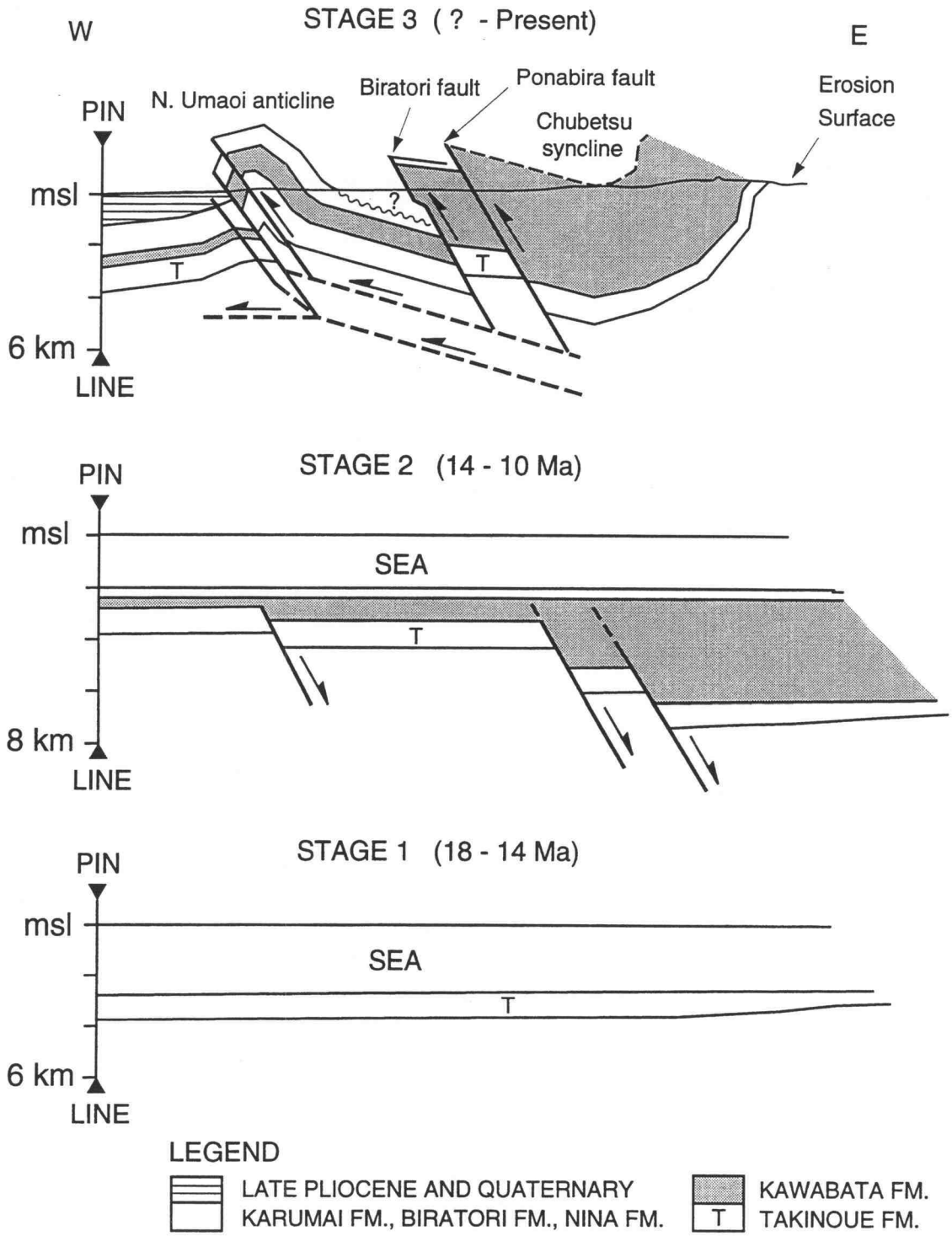

Figure 11 Three-stage retrodeformation model based on interpretation of syndeformational growth strata and balancing of cross section A-A'. Structure of underlying thrust in pre-Neogene rocks is speculative.

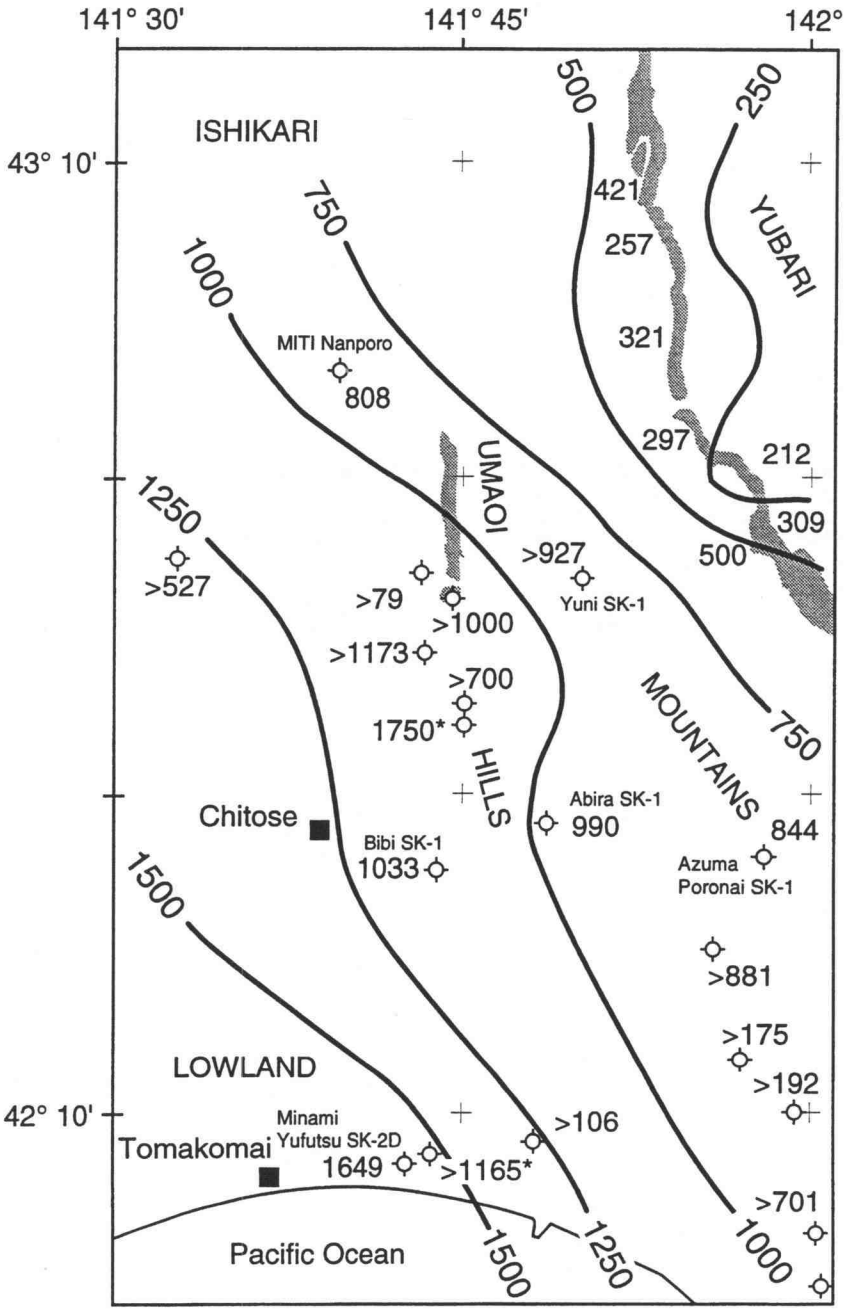

Figure 12 Isopach map of the Takinoue Formation. Numbers indicate stratigraphic thicknesses at outcrops (shaded) and in oil wells. Drillholes in which faulting has overthickened the stratigraphic section are marked by an asterisk.

Middle Miocene Extension (Stage 2)

The major reverse faults of the Yubari Fold and Thrust Belt are reactivated middle Miocene normal faults. Consequently, shortening and reverse separation across these faults are several times greater in Karumai and younger strata than in underlying strata. This relationship is best documented on the Biratori Fault, where reverse separation of the top of the Kawabata is 3,250 m (2,600 m minimum), and reverse separation of the underlying Takinoue is only 875 m (Figure 13a). Palinspastic removal of reverse separation at the top of the Kawabata leaves 2,150 m of normal separation of the Takinoue. This amount of normal separation equals the thickness increase of the Kawabata across the fault. Hence, the thickness increase is a direct result of normal slip on the Biratori Fault during deposition of the Kawabata Formation.

Isopachs of the Kawabata show a regional correlation between thickness changes and the location of major faults (Figure 14). Abrupt eastward increases in thickness are coincident with the Yufutsu, Umaoi, Biratori, and Ponabira Faults and are continuous along strike. Hence, these faults divide the region into elongate blocks of uniformly thick Kawabata and define the western margin of a codepositional structural graben. Gradual thickness changes within blocks along fault strike appear to reflect decreasing slip toward the terminal ends of normal faults.

Subsurface data suggest the existence of a buried normal fault, the Yufutsu Fault, in the Ishikari Lowland consistent with middle Miocene extension (Figure 13b). Subhorizontal reflectors on an industry seismic

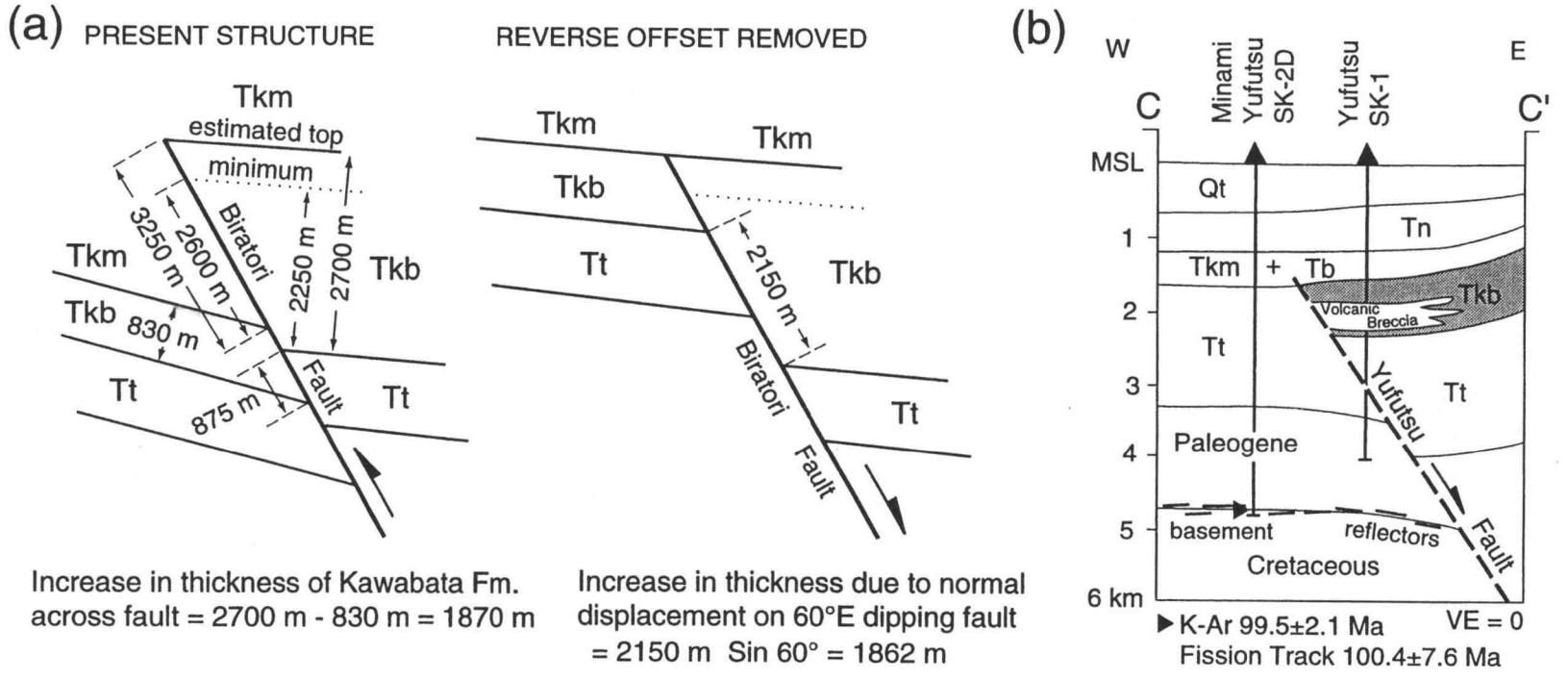

Figure 13 (a) Palinspastic reconstruction showing that middle Miocene normal slip on the Biratori Fault accounts for increase in stratigraphic thicknesses of Kawabata Formation across the fault. (b) structure section of the Yufutsu Fault based on drillcore biostratigraphy (Okamura et al., 1992; Niitsuma et al., 1982) and an industry seismic-reflection profile (Mitani, 1978). Section location shown in Figure 3.

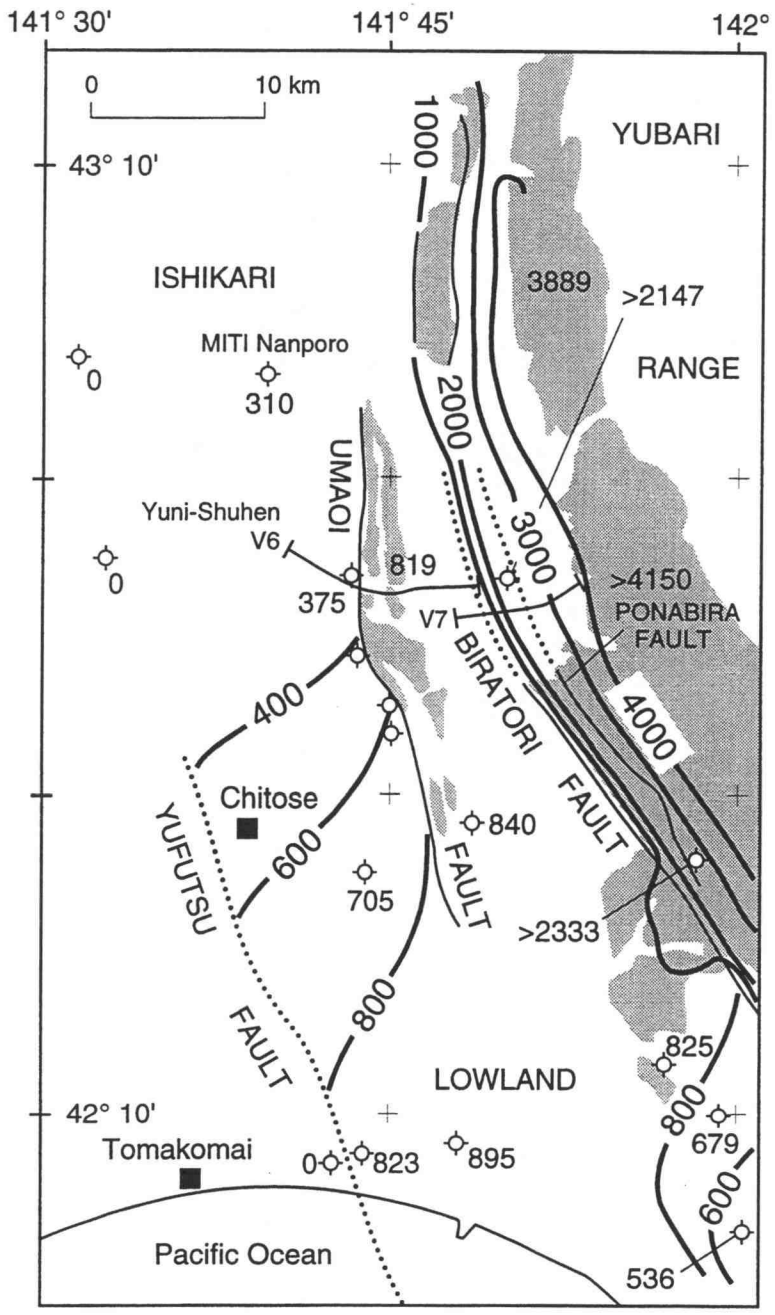

Figure 14 Isopach map of the Kawabata Formation in relation to major faults. Numbers indicate stratigraphic thicknesses at outcrops (shaded) and in oil wells. Abrupt eastward increases in stratigraphic thickness at faults indicate control by coeval normal faulting.

reflection profile and drillcore biostratigraphy from Yufutsu SK-1 and Minami Yufutsu SK-2D indicate that the Kawabata Formation terminates in the vicinity of the Yufutsu Fault and that the Takinoue Formation is displaced vertically by about 800 m (Mitani, 1978; Niitsuma et al., 1982; Okamura et al., 1992). The absence of Kawabata in Minami Yufutsu SK-2D suggests it was deposited on the downthrown side of a growth normal fault, while a localized sill of volcanic breccia in Yufustu SK-1 suggests the fault served as a magma conduit. A distinct top-of-basement reflector, which correlates with Cretaceous granitic rock in Minami Yufutsu SK-2D, exhibits an east side down vertical separation and constrains the dip of the fault to the east (Mitani, 1978).

Post-late Miocene Compression (Stage 3)

Wedges of growth strata on the flanks of the Umaoi Hills record compressional deformation associated with uplift of the Northern Umaoi Anticline (Figure 8). A triangular zone of 2° east-dipping reflectors between the Biratori Fault and the eastern rangefront of the northern Umaoi Hills onlaps underlying 15° east-dipping reflectors, forming an angular unconformity of about 12°. Depositional slopes of modern submarine fans range between 1° and 7° (Normark et al., 1993); hence, this angular discordance is too large to be purely depositional. Thus, the unconformity indicates a period of tectonic rotation, sometime after deposition of the Karumai Formation at about 9 Ma, in which the east limb of the Northern Umaoi Anticline tilted 12° to the east.

A similar wedge of growth strata in the footwall of the Umaoi Fault implies that structural growth of the Northern Umaoi Anticline began in the early to middle Pliocene (Figure 8). Reflectors correlative with early Pliocene and Miocene strata in Nishi Umaoi SK-1 are subparallel, defining a sedimentary sequence of uniform thickness. In contrast, seismic reflectors above the Nina Formation converge defining a sedimentary wedge that conforms to the structural upwarp of the footwall, tapering from 1,250 m in the Ishikari Lowland to 350 m at the rangefront of the Umaoi Hills. Upper Nina Formation exposed along the western rangefront contains rip-up blocks of siltstone up to 50 meters in diameter. The size of these blocks indicates that they have not been transported very far from their source area, and suggests that they are derived from uplifting bedrock in the northern Umaoi Hills during the early Pliocene.

SHORTENING

Shortening and extension across the Yubari Fold and Thrust Belt are estimated from bed-length measurements using the structural configuration shown in Stage 3 of the retrodeformation model (Figure 11). Both the hypothetical structural geometry constructed for the eroded part of the Northern Umaoi Anticline and the reconstructed top of the Kawabata Formation in the Chubetsu Syncline result in minimum bed-length values. Thus, assuming that the Kawabata underwent parallel folding without significant internal or ductile deformation, the amounts of shortening and extension predicted by the model are minimum estimates.

Bed-length measurements on the upper contact of the Kawabata indicate that the total shortening across the Yubari Fold and Thrust Belt is approximately 7 km, or 25%. Combining this shortening estimate with the 9 to 4.5 Ma age for onset of compressional deformation interpreted from growth strata yields a first-order, long-term-average shortening rate estimate of 0.8 to 1.6 mm/year. Measurements on the lower contact of the Kawabata indicate that the total shortening is about 5 km. This difference in shortening of stratigraphic markers above and below the Kawabata Formation demonstrates that about 2 km of extension occurred during the middle Miocene in Stage 2 of the retrodeformation model.

LATE QUATERNARY TECTONICS

Late Quaternary deformation along the structural boundary between the Ishikari Lowland and the Yubari Fold and Thrust Belt is limited to secondary structures overlying blind faults (Research Group for Active Faults of Japan, 1991). West of the Kurisawa Hills, an east-facing fault scarplet offsets the surface of a marine terrace, and along the northern Umaoi Hills this terrace is tilted 1.5° to the west (Okumura, 1987; Research Group for Active Faults in Japan, 1991; Figures 3 and 6). This terrace correlates with oxygen-isotope stage 5e or 5c, based on the presence of the Toya Ash tephra and marine diatoms in underlying sediments, and therefore formed at 100-120 ka. West of the southern Umaoi Hills, a series of range-facing scarplets up to 4 m high offset a pyroclastic ash flow from Shikotsu volcano, radiocarbon dated at circa 31 ka (Katsui, 1959; Arai et al., 1986).

Deformation of the Late Pleistocene Gravel Fan

The Abira Formation along the Yubari and Abira Rivers was correlated with gravel occupying a low saddle in the central Umaoi Hills and buried beneath marine sediment in the Ishikari Lowland on the basis of field exposures, drillcore data, a high-resolution seismic-reflection record, and geomorphic relationships interpreted from aerial photographs (Geographical Survey Institute of Japan, 1974). These gravels are part of a broad alluvial fan deposited at the rangefront of the Yubari Mountains (Figure 15). The constructional top of the gravel fan forms a conspicuous geomorphic surface characterized by flat-topped ridges and a dense network of incised drainage

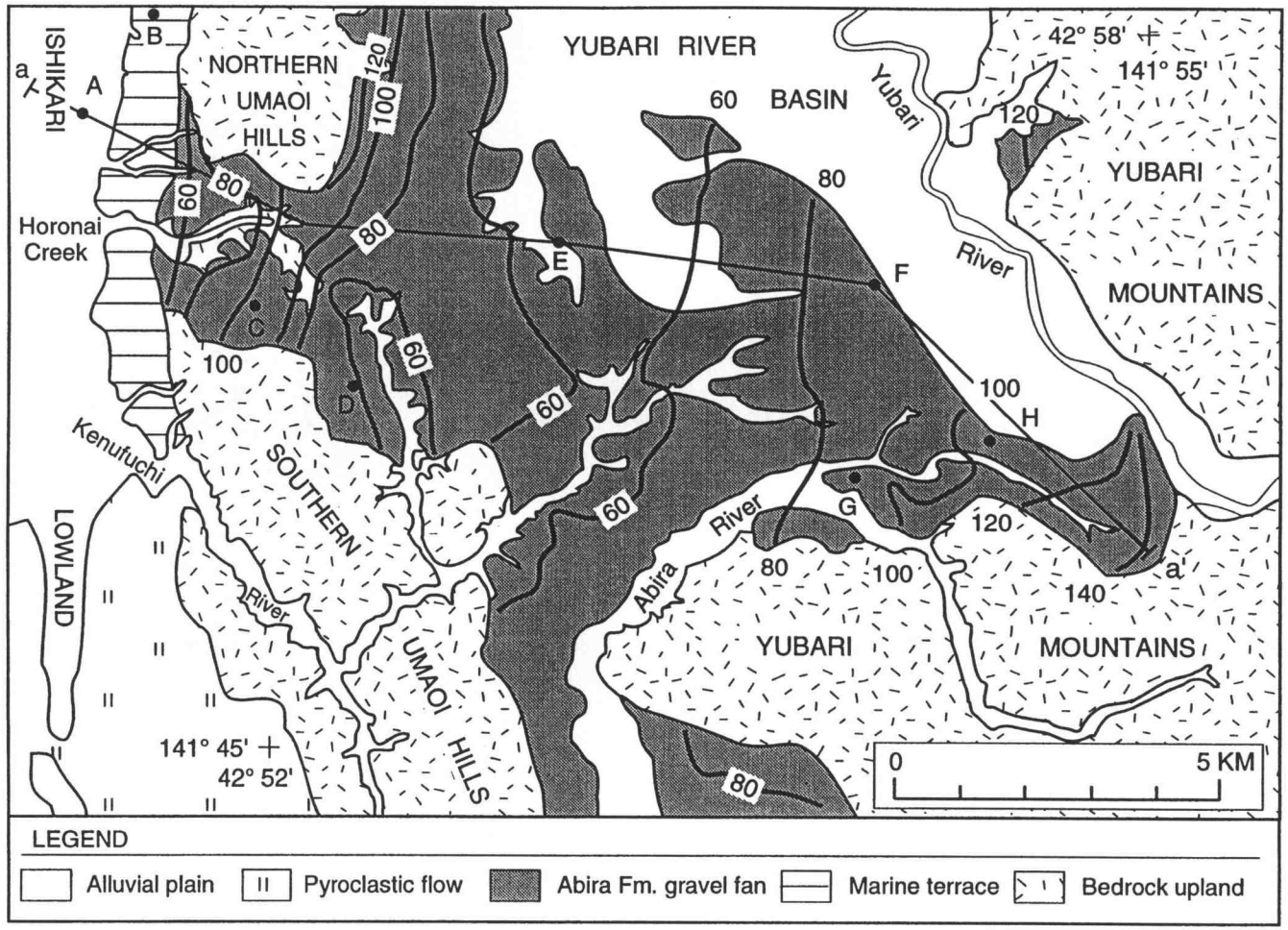

Figure 15 Surficial deposits and geomorphic surfaces in the central Umaoi Hills. Structure contours approximate the constructional top of the Abira gravel fan. Section a-a' was used to construct the longitudinal profile of the fan in Figure 7. Map location is shown in Figure 3.

gullies. Structure contouring of the ridgetop altitudes provides an approximation of the constructional surface.

Structure contours on the top of the Abira Formation show that the constructional surface of the gravel fan is arched over the Umaoi Hills (Figure 15). The longitudinal profile in Figure 7 shows the geometry of this deformed surface based on structure contours and the correlations in Figure 5. The undeformed depositional geometry was estimated using an empirical relationship between clast size and fan slope (Boothroyd and Nummedal, 1978). This relationship was derived from modern climatic and environmental analogs to the Abira fan associated with coastal braided-river systems in Iceland and Alaska, U.S.A. These analogs indicate that the depositional slope of the Abira fan was 6±2 m/km and suggest that the head of the fan, with an average slope of 5.3 m/km, is undeformed.

Active Structures

Northern Segment of the Umaoi Fault

In the middle to late Pleistocene, the main strand of the Umaoi Fault became inactive, and a new strand of the fault began to form about 1 km to the west. Although the main strand of the fault cuts Quaternary sediment and controls the rangefront of the northern Umaoi Hills, this strand does not offset the 100-120 ka marine terrace (Figures 6 and 9). In contrast, seismic reflectors overlying the western strand of the fault at a depth of about 200 m are upwarped directly above the fault tip, exhibiting 100 m of relief over a distance of 0.5 km (Figure 16). In record Yuni-Shuhen V6, deeper reflectors

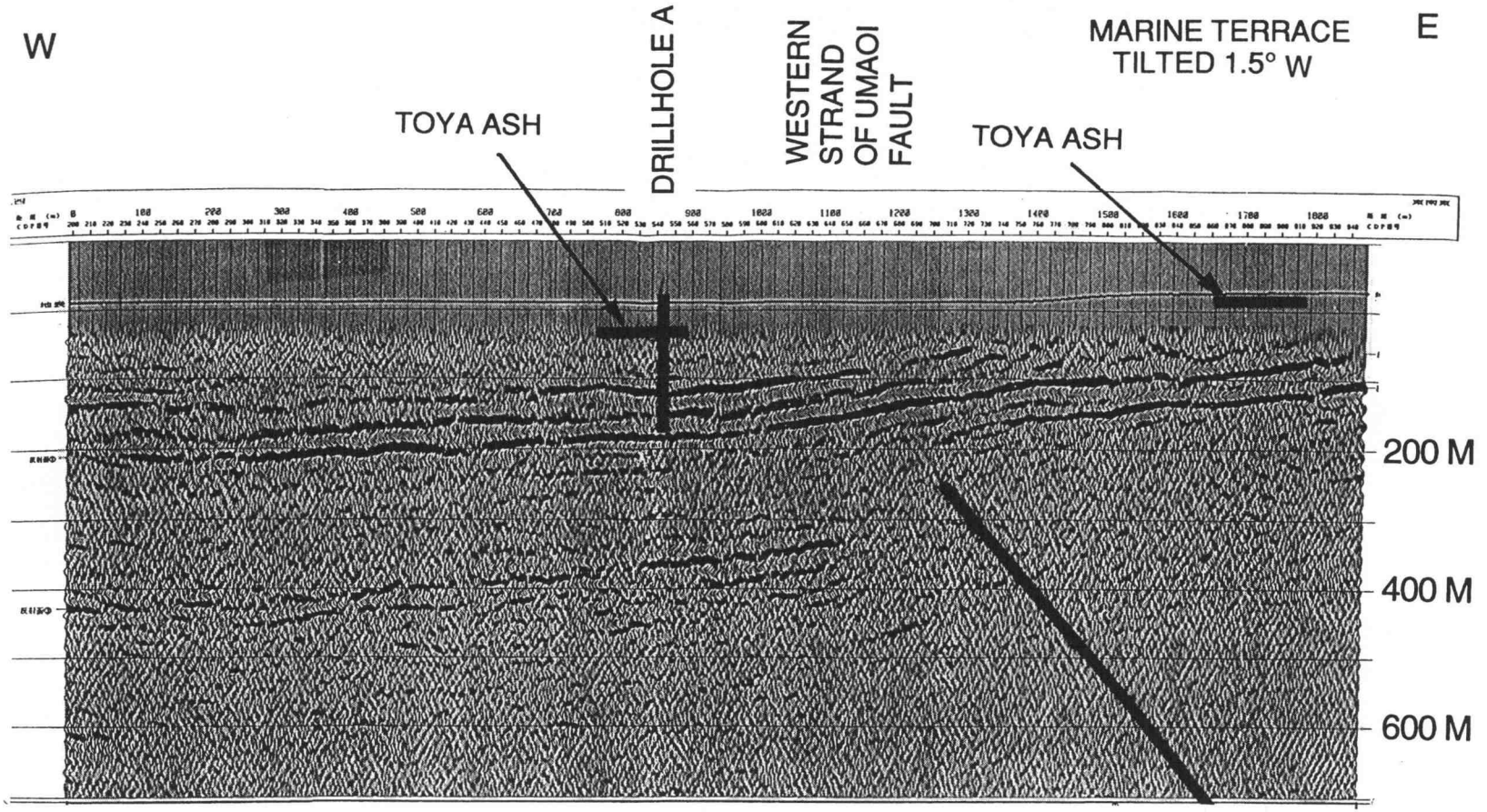

Figure 16 High-resolution, migrated, seismic-reflection depth record acquired by the Geological Survey of Japan in 1992 across the northern segment of the Umaoi Fault zone. Drillhole A, marine terrace exposure, and western strand of Umaoi Fault from seismic-reflection record Yuni-Shuhen V6 are plotted on record. Reflectors correlated with late Quaternary sediment in drillhole A upwarp above tip of projected fault. Vertical separation of Toya Ash is used to calculate a slip rate for the fault at depth. Location of line shown in Figure 6.

that are subhorizontal beneath the Ishikari Lowland at 0.3-0.6 seconds upwarp sharply at the fault, tilting to ~25° E (Figure 8).

Overlying the reflectors are marine sediment and tephra deposited in a shallow, quiet-water embayment that occupied the Ishikari Lowland in the late Pleistocene. Cyclic interlayering of fine sand, silt, and peat, containing marine, brackish-water, and fresh-water diatoms indicate that these sediments represent a tidal-flat environment subject to a fluctuating sea level (Figure 5). East of the upwarp, Toya Ash lies within silt interlayered with sand and peat that underlies the marine terrace along the northern Umaoi Hills. On the west, Toya Ash is identified in the same sediments, in drillhole A, at an altitude 29.5 m lower than in the marine terrace exposure. Inference that the Toya Ash came to rest on a near-horizontal tidal flat yields a reverse slip-rate estimate of 0.41±0.04 mm/yr for the western strand of the fault. Hence, reverse slip on this fault accounts for 0.26±0.03 mm/yr of east-west convergence.

This estimate is dependent upon the assumption that the Toya Ash blanketed a near-horizontal tidal flat that included the two tephra localities. Relief on the Toya Ash could be attributed to the existence of a terrace riser in the 0.8 km distance between the two tephra localities, analogous to the 8-m-high riser that exists today between the Ishikari Lowland and the marine terrace. However, this scenario is unlikely, because (1) deposition of the Toya Ash was preceded by 20 m of transgressive sedimentation at locality A that would have buried any terrace risers between the two sites, and (2)

development of a 2-m-thick cap of peat on the transgressive sequence implies that the shoreline associated with the next younger stable lowstand was located west of drillhole A (see Figure 5).

Northern Umaoi Hills Arch

Warped geomorphic surfaces indicate that the northern Umaoi Hills are actively uplifting and suggest that this topography is largely a result of late Pleistocene uplift. The Abira gravel fan forms a 5-km-wide arch that matches the topography of the central Umaoi Hills (Figures 7 and 15). Along the western rangefront of the northern Umaoi Hills, the surface of the 100-120 ka marine terrace tilts westward at an angle of 1.5°. This tilt is inferred to be tectonic, because (1) the terrace deposits are primarily silt, fine sand, and peat, indicative of a flat-lying, tidal marsh environment (Okumura, 1987), and (2) the terrace surface is near-horizontal at the nose of the anticline.

Comparison of the arched fan profile to the estimated depositional geometry indicates that anticlinal arching has uplifted the northern Umaoi Hills by 60 to 82 m (Figure 7). The minimum age for abandonment of the constructional surface, given by the Kc-Hb tephra, is 110±10 ka; thus, the rate of uplift in the northern Umaoi Hills is at least 0.66±0.17 mm/year. The rate of uplift is probably greater to the north of the profile location in the more central part of the hills, because the Abira Formation there extends to an altitude greater than 120 m (Figure 15).

Geometric and temporal associations suggest that the Northern Umaoi Hills Arch is a fault-propagation-fold related to blind reverse faulting on the western strand of the Umaoi Fault. The crest of the arch does not correspond with the fold axis of Northern Umaoi Anticline and, therefore, the arch does not reflect continued growth the Neogene structure. Similarly, the western margin of the arch does not coincide with the main strand of the Umaoi Fault, but instead coincides exactly with the western strand of the fault. Hence, development of a new axis of folding in the northern Umaoi Hills seems related to the shift in the locus of faulting from the main strand of the Umaoi Fault to the western strand.

Drainage Response to Tectonic Uplift

Rapid tectonic uplift of the northern Umaoi Hills forced the ancestral Kenufuchi River to abandon a throughgoing channel across the central Umaoi Hills and seek a new course to the south (Figure 17a). A 0.5-km-wide wind gap incised into Abira gravel at the crest of the Northern Umaoi Hills Arch connects the head of the north fork of the modern Kenufuchi River with the head of Horonai Creek. The headwaters of these two streams are underfit; hence, the north fork of the Kenufuchi River must have flowed west through the wind gap and along Horonai Creek. The absence of Abira gravel in the lower half of the modern Kenufuchi River drainage indicates that the modern course is younger than the gravel. If this channel had existed at the time of gravel deposition, it would have served as the primary conduit for gravel transport across the Umaoi Hills.

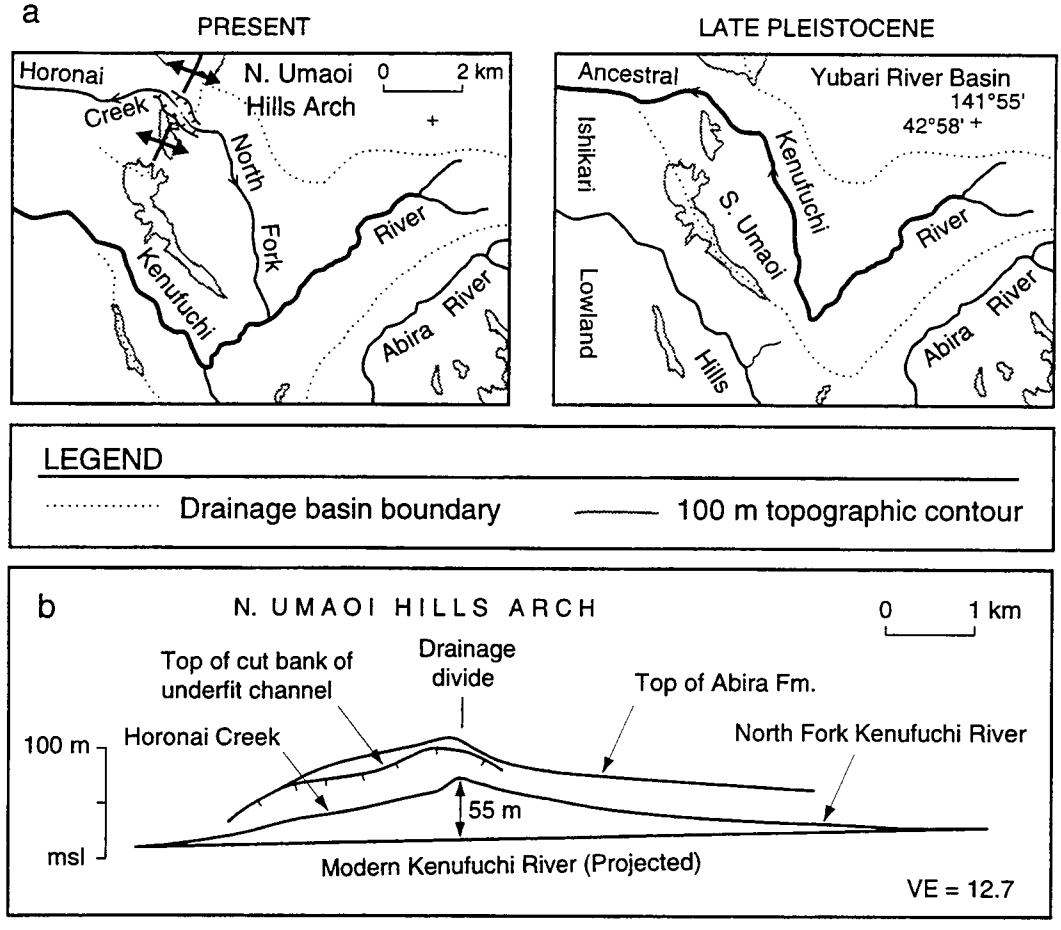

Figure 17 (a) Stream capture of the Kenufuchi River due to rapid arching of the northern Umaoi Hills. (b) Thalweg profile of the late Pleistocene channel of the Kenufuchi River now occupied by underfit streams: Horonai Creek and the North Fork of the Kenufuchi River. The top of the Abira Formation, the channel profile, and the top of the cutbank all exhibit similar folding geometry over the crest of the Northern Umaoi Hills Arch. Comparison of the late Pleistocene channel to the modern profile indicates at least 55 m of uplift has occurred since stream capture.

In Figure 17b, the arched geomorphic surface of the Abira gravel fan is plotted in relation to the longitudinal profiles of the ancestral and modern channels of the Kenufuchi River. The profile of the abandoned channel coincides closely with the constructional top of the Abira Formation suggesting that the channel profile is largely controlled by tectonic uplift. Folding of the top of the cutbank of the abandoned channel is especially convincing. The amount of relief between the old and new courses of the Kenufuchi River is 55 m, slightly less than the estimated uplift of the gravel fan. These geomorphic parameters support the conclusion that rapid uplift of the Northern Umaoi Hills Arch defeated the late Pleistocene course of the Kenufuchi River, and caused the river to shift southward to its present location.

DISCUSSION

This study shows that the Yubari Fold and Thrust Belt was a site of middle Miocene normal faulting and proposes that these normal faults are part of a previously unrecognized failed crustal rift (Figure 18). The rift is expressed as a 1000-km-long and 60-km-wide basin that contains an extremely thick (5-8 km) section of Cenozoic sediments. This linear basin includes the West Sakhalin Trough at the eastern margin of Tartar Strait in the Russian Far East and continues onland as the Ishikari-Teshiro Belt in west-central Hokkaido (Antipov et al., 1980; Fournier et al., 1994).

Many of the synrift structures were reactivated or deformed during subsequent strike-slip or contractional tectonics, thereby masking the origin of the rift basin. The offshore part of basin has been interpreted as an expression of strike-slip faulting (Lallemand and Jolivet, 1986; Fournier et al., 1994), whereas the onshore part has been interpreted as an expression of oblique collision and crustal underthrusting (Okada, 1983; Hoyanagi et al., 1986; Kimura and Miyashita, 1986). The unusually narrow width and northerly trend of the rift zone may reflect the influence of inherited structures, including Paleogene strike-slip faults, that provided preexisting zones of crustal weakness.

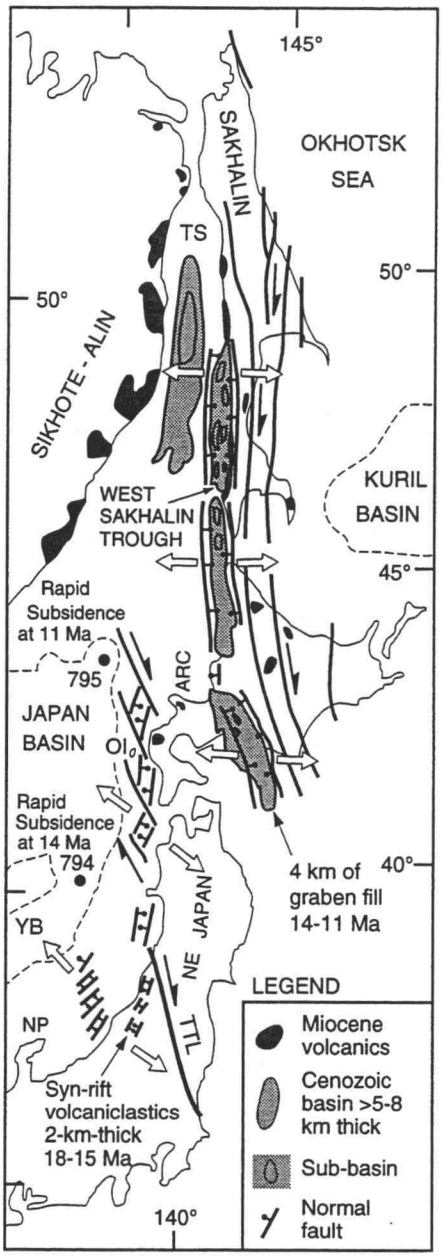

Figure 18 Proposed middle Miocene crustal rift as delineated by known tectonic and geologic features. Open arrows denote direction of extension. Early Miocene rift zone along western northeast Japan is after Fournier et al. (1994) and Yamaji (1990). Miocene volcanics from Antipov et al. (1980), Zonenshain et al. (1990), and Geological Survey of Japan (1992). NP - Noto Peninsula, OI - Okushiri Island, TTL - Tanakura Tectonic Line, TS - Tartar Strait.

Ishikari-Teshiro Belt

The Ishikari-Teshiro Belt in Hokkaido consists of two Neogene depocenters (Okada, 1983), the Teshiro-Haboro Basin and the Ishikari-Yubari Basin (Figure 19). Middle Miocene gravity-flow and shallow-marine deposits similar to the Kawabata Formation are more than 4 km thick, and consist mostly of coarse- to fine-grained turbidites and contourites derived from source areas to the east in central Hokkaido (Okada, 1978, 1983; Hoyanagi et al., 1986). Paleocurrent indicators and facies of submarine fans indicate that these sediments were deposited a rapidly subsiding, north-trending, bathymetric trough (Hoyanagi et al., 1986). The landmass-parallel trend of submarine fans is unusual and indicates that some form of bathymetric boundary on the west side of the basin blocked westward migration of the turbidite fans.

Teshiro-Haboro Basin

The Teshiro-Haboro Basin is a north-trending, 175-km-long and 60-km-wide basin (as defined by Neogene sediments greater than 1-km-thick) containing more than 5 km of Neogene sediment (Figure 19). On the east, the basin is bounded by the Horonobe Fault in northern Hokkaido (Geological Survey of Japan, 1992), while the western half of the basin lies on the continental shelf (Okada, 1983). Okada (1978) described north-trending sub-basins in the Teshiro-Haboro Basin containing chaotic breccias and suggested that these detrital influxes were associated with NNW-trending thrust and reverse faults that seem to control the sub-basin boundaries.

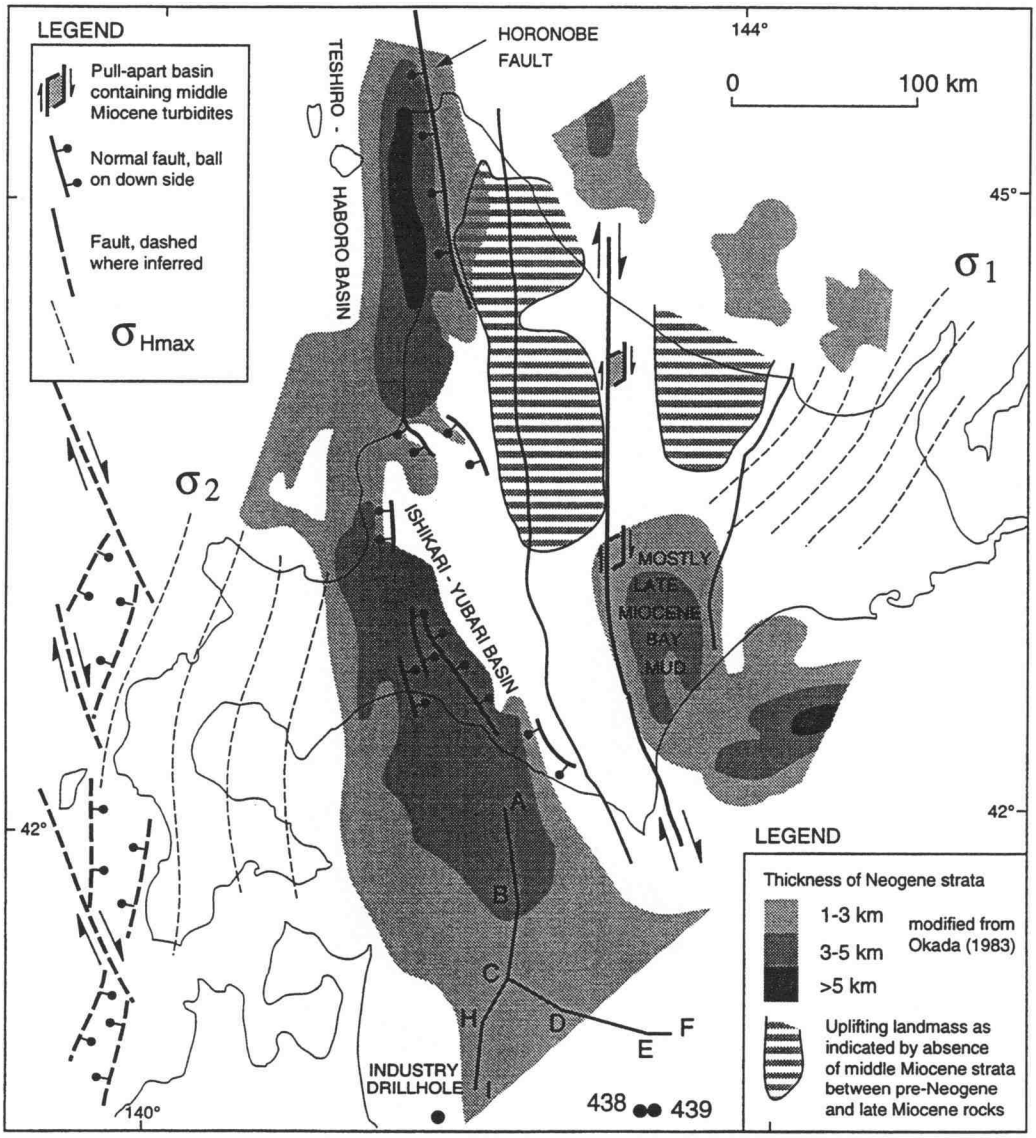

Figure 19 Middle Miocene tectonic features of Hokkaido. Thick Neogene strata in western Hokkaido are primarily middle Miocene turbidites. This sediment was supplied from a rapidly uplifting landmass in north-central Hokkaido deduced from fossil, shoreline facies, and provenance data (Hoyanagi et al., 1986; Chinzei, 1986). In eastern Hokkaido, middle Miocene turbidites are found within small (~3-km-wide, >10-km-long) pull-apart basins along strike-slip faults. Offshore faults after Fournier et al. (1994) are inferred to be early Miocene.

Ishikari-Yubari Basin

The Yubari-Ishikari Basin (Figure 19) is a NNW-trending, elongate basin of Neogene sediment 3-5 km thick that extends from latitude 43.5° to about 41° (Okada, 1983). North- and northwest-striking reverse faults onshore divide the basin into two sub-basins: the Ishikari Basin, a younger, western basin associated with east-west compression and containing mostly post-middle Miocene sediment, and the Yubari Basin, an older, eastern basin associated with extension and containing mostly middle Miocene turbidites and contourites (Figure 7).

Collision-Flexure Model

Current models postulate that thick sedimentation in the Ishikari-Teshiro Belt was associated with a tectonic collision between western and eastern Hokkaido (Den and Hotta, 1973; Kimura et al., 1983; Okada, 1983; Kimura and Miyashita, 1986; Hoyanagi et al.,1986; Lallemand and Jolivet, 1986). Hoyanagi et al. (1986) and Kimura and Miyashita (1986) modeled the middle Miocene basin as a "frontal depression" that formed above a crustal flexure in the Eurasian Plate caused by oblique collision and overthrusting of the North American Plate. This model is analogous to the Taranaki Basin in New Zealand, where oceanic crust is thrust beneath an island arc, and thrust faults bound an asymmetrical wedge of sediment (Holt and Stern, 1994).

There are two principal shortcomings to the collision-flexure model. The first is that the middle Miocene basins in the Ishikari-Teshiro Belt are too narrow to be a reflection of crustal flexure. Crustal flexures, such as the Taranaki Basin in New Zealand, the foreland basin of the Himalayan thrust

front, and the subduction zones of the Pacific Rim, form broad depressions on the order of 100 to 200 km wide before achieving 4 km of structural relief (Hilde, 1983; Lillie et al., 1987; Holt and Stern, 1994). In contrast, the Teshiro-Haboro Basin, as defined by Neogene sediment greater than 1 km thick, is only 60 km wide (Okada, 1983). Similarly, in the Ishikari-Yubari Basin, middle Miocene sediment thicken at rate 4 to 8 times greater than the gradient of thickening in the flexure basins cited above (before post-late Miocene shortening).

Another problem is that the model requires simultaneous, large-scale normal and thrust faulting on opposite sides of the Yubari Basin. Bending-moment normal faults in flexing crust coeval with thrust faults in accretionary wedges are well documented at subduction zones of the circum-Pacific region, but these normal faults exhibit total vertical displacements of less than 500 m and dip directions that alternate in a classic horst and graben pattern (Hilde, 1983; von Huene, et al., 1986; von Huene and Culotta, 1989; von Huene and Scholl, 1991). Normal faults defining the western margin of the graben in the Ishikari-Yubari Basin exhibit much larger normal separations (800-1,700 m) and are systematically east-dipping. Hence, crustal flexure is not a satisfactory explanation for the origin of these faults.

Seismic Refraction Data

Deep Sea Drilling Project (DSDP) drillholes and seismic-refraction profiles show that the general crustal structure of the northeast Japan forearc consists of three layers: 1.6-3.5 km/s sediment of Pleistocene to Paleogene age overlying 3.6-5.1 km/s Cretaceous age material, which in turn overlies 5.8-6.2

km/s continental crust (Ludwig, 1966; Murauchi and Ludwig, 1980; Nagamo et al., 1980; von Huene et al., 1982). Figure 20 shows two crustal velocity sections, A-B-C-H-I and C-D-E-F, that cross the offshore extension of the Ishikari-Yubari Basin (Asano et al., 1979). Industry drillholes indicate that the 2.9 km/s and 4.2-4.4 km/s layers at I-H correlate with Paleogene strata overlying Cretaceous volcanic, basic igneous, and sedimentary rocks, including chert and limestone (von Huene et al., 1982). At E-F, DSDP drillholes 438 and 439 show that the 4.8 km/s layer is Cretaceous sediment, whereas the overlying 1.7-2.6 km/s layers correspond mostly to Neogene sediment.

On A-B-C-H-I, the Ishikari-Yubari Basin is expressed as a 6-km-thick zone of 1.7-3.5 km/s velocities, representative of Tertiary sediment. Industry isopachs indicate 3-5 km of this sediment sequence is Neogene (Okada, 1983). By analogy with the onshore part of the basin, the 3.1-3.5 km/s layer and some of the overlying 1.7 km/s layer are interpreted as synrift sediment correlative with the Kawabata Formation in the Yubari Basin. Thickening of the 3.1-3.5 km/s layer is compensated for by substantial thinning of the underlying 4.2 - 5.1 layer, whereas at E-F and I-H, where the 4.2-5.1 km/s layer is not thinned, the 3.1-3.5 km/s layer is absent. These structural geometries imply that the Neogene basin and thinning of the underlying crustal layer are intimately related. Farther south, away from the deepest part of the Neogene basin at C-D, the 4.8 km/s layer is continuous and shows that thinning of this layer is limited to the basin.

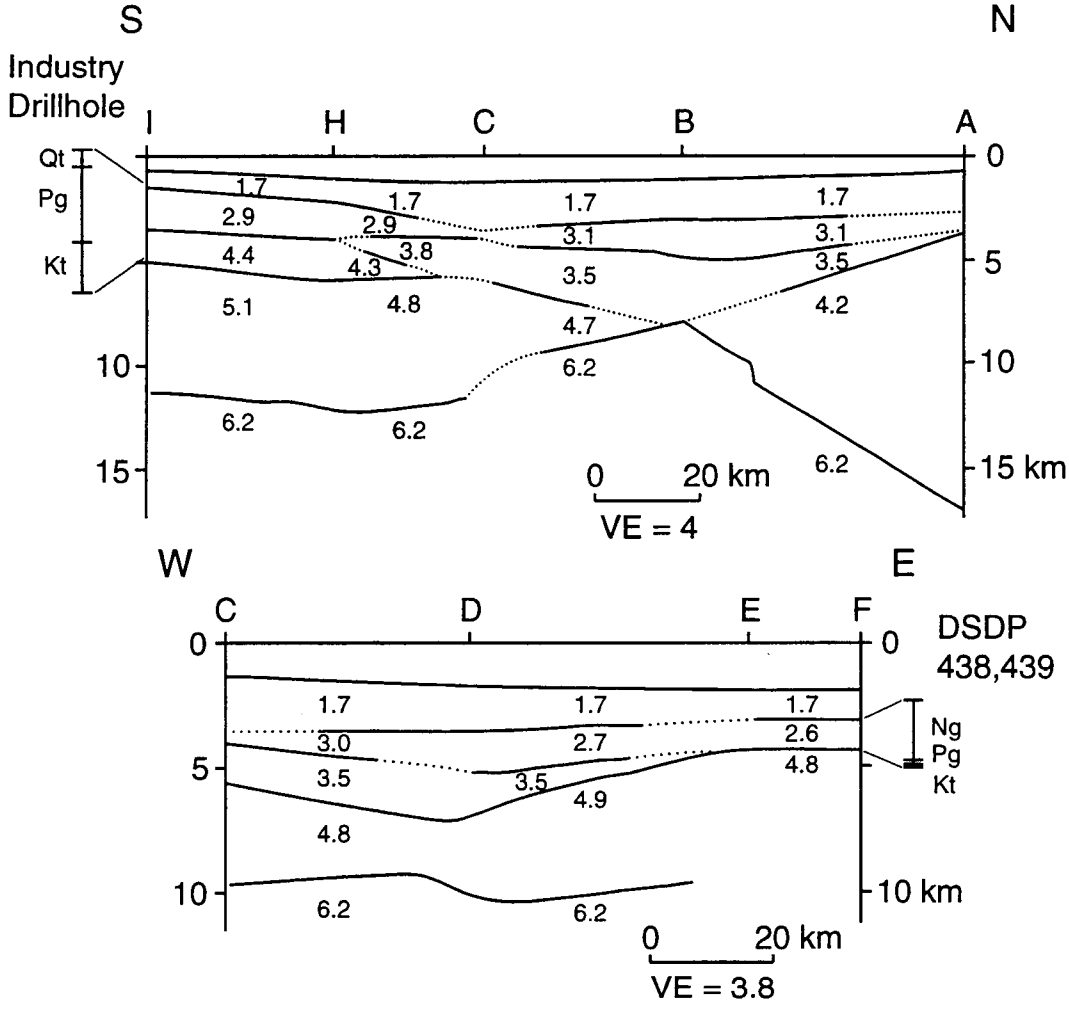

Figure 20 Crustal velocity sections across the offshore extension of the Ishikari-Yubari Basin constructed from seismic refraction measurements of P-wave velocities in km/sec at lettered sites from Asano et al. (1979). Correlations between drillholes and velocity layers are plotted at ends of sections. Section lines and drillhole locations are shown in figure 19.

Hence, a logical conclusion is that crustal extension associated with graben formation in the Yubari-Ishikari Basin thinned the 4.2-5.1 km/s layer. The 4.2-5.1 km/s layer correlates with a north-trending Cretaceous subduction complex extending across western and central Hokkaido (Kiminami and Kontani, 1983). At A-B, the 4.2 km/s layer correlates with Cretaceous turbidites in west-central Hokkaido (the Yezo Group) that rest on blueschist and ophiolite (the Soruchi Group), emplaced as imbricate thrust sheets in an accretionary complex (Ishizuka et al., 1983, *in* Jolivet and Huchon, 1989). Contemporary rocks in western Hokkaido are island-arc type lithologies consisting mostly of andesitic volcanics, clastic sediments, and granitic intrusions (Kiminami and Kontani, 1983). Thinning of the 4.2-5.1 km/s layer is enigmatic in the framework of a subduction complex, so it is unlikely that this feature is a Cretaceous structure.

Within the thinned zone, the lowermost crustal layer of velocity 6.2 km/s protrudes several kilometers upward and is shown in contact with the 3.5 km/s layer. An attractive interpretation is that the protrusion is a shallow magma chamber and is the source of the intrusive volcanics found within the pre-late Miocene strata of the Ishikari-Teshiro basin, including the central Umaoi Hills and drillholes Miti-Nanporo, Yufutsu SK-1, and Kyowa SK-1. Another possible interpretation is that the protrusion is some kind of positive flower structure created during Paleogene strike-slip faulting; however, this interpretation does not explain the close spatial correspondence between the Neogene basin and the thinned Cretaceous layer.

Synrift Deformation

Sedimentologic evidence demonstrates that the style of tectonic deformation changed in the middle Miocene to deformation characterized by coupled subsidence of the Ishikari-Teshiro Belt and uplift of central Hokkaido (Okada, 1983; Hoyanagi et al., 1986). In the Ishikari-Yubari Basin, the change from slow sedimentation of silt on a marine shelf, represented by the Takinoue Formation, to rapid deposition of thick turbidites and contourites indicates a sharp acceleration in the uplift rate of central Hokkaido, which was already partly emergent in the early Miocene (Chinzei, 1986). Petrographic and lithologic studies indicate that the middle Miocene turbidites were derived from erosional sources in a rapidly uplifting central Hokkaido (Okada, 1983; Kimura et al., 1983; Hoyanagi et al., 1986). Paleostress data show that the orientation of σ_{Hmax} remained NE-trending until the late Miocene (Kimura, 1981); therefore, the shift to vertical tectonics in the middle Miocene can not be explained as a clockwise rotation of σ_1.

Late early Miocene and middle Miocene rocks in the Ishikari-Yubari Basin exhibit a substantially lower grade of deformation than the Paleogene rocks that they overlie with angular unconformity or disconformity (Hata, 1964; Ishida et al., 1980). Early Miocene, Paleogene, and Cretaceous rocks are strongly deformed by structures indicative of dextral transpression (Jolivet and Huchon, 1989). In contrast, structures in the late early and middle Miocene Takinoue and Kawabata Formations reflect primarily east-west extension and contraction. Citing fault-set data from northern Hokkaido and the Hidaka Mountains, Jolivet and Huchon (1989) and Fournier et al. (1994) conclude that transpressional deformation continued until the end of the

middle Miocene. However, their conclusion seems speculative for southern Hokkaido, because aside from the Ishikari-Teshiro Belt, middle Miocene rocks are largely absent. Hence, the assemblage of structures in the Yubari Fold and Thrust Belt is more consistent with transtensional or extensional deformation in the middle Miocene.

A similar argument can be made for the northern part of the Ishikari-Teshiro Belt. The 120-km-long Horonobe Fault (on land) controls the eastern margin of the Teshiro-Haboro Basin, across which Neogene sediment thickens westward from 1 km to greater than 5km (Okada, 1983; Figure 19). A geologic map shows that the sharp increase in thickness of Neogene sediment takes place in middle Miocene turbidites on the west side of the fault (Geological Survey of Japan, 1992). The map also shows that the Horonobe Fault juxtaposes Pliocene strata on the west against Miocene strata on the east with little vertical separation of late Miocene strata. These relationships suggest that a west-side-down separation of several kilometers occurred on the Horonobe Fault during the middle Miocene.

In the collision-flexure model, west-side-down separation on the Horonobe Fault is attributed to middle Miocene thrust faulting, but most of the structures in the middle Miocene strata are associated with post-middle Miocene dextral strike-slip motion on the Horonobe Fault (Kimura et al., 1983). NNW-striking, en echelon, right-stepping fold axes and thrust faults (Sylvester, 1988), and clockwise paleomagnetic rotation of the Oligocene to early Miocene (30°±21°) and middle Miocene (20°±15°) rocks (Kodama et al., 1993) indicate that these structures resulted from dextral shear, while the gentle to open grade of folding (Kimura et al., 1983) in middle Miocene to

Pliocene strata suggest that most of the deformation is post-middle Miocene. Thus, the large west-side-down separation on the Horonobe Fault seems more consistent middle Miocene normal faulting and later reactivation as a strike-slip fault.

Paleostress Field

Paleo-stress fields in northern Japan are reconstructed from the orientation of dikes, veins, fold axes, and faults (Figure 19). In the late Miocene, the stress field of northern Honshu and southwestern Hokkaido changed from an extensional regime with $\sigma_{Hmax} = \sigma_2$ trending N-NNE to a compressional regime with $\sigma_{Hmax} = \sigma_1$ trending east-west (Nakamura and Uyeda, 1980; Sugi et al., 1983; Yamagishi and Watanabe, 1986). In eastern Hokkaido, the stress field also shifted in the late Miocene, but from a stress regime with σ_{Hmax} trending NE to a stress regime of east-west compression with $\sigma_{Hmax} = \sigma_1$ (Kimura, 1981). The middle Miocene NE-trend of σ_{Hmax} in eastern Hokkaido is interpreted to be σ_1 based on the formation of pull-apart basins containing middle Miocene turbidites in N-trending strike-slip fault zones that offset a granitic body K-Ar dated at 15 Ma (Watanabe and Iwata, 1985; Kimura and Miyashita, 1986; Jolivet et al., 1992). Similarly, Fournier et al. (1994) used structures deforming middle Miocene volcanics intruded along the Tym-Poronaysk Fault in Sakhalin to deduce coeval east-west contraction and dextral strike-slip motion with σ_1 trending N50°-90°E. Hence, the middle Miocene stress field of eastern Hokkaido seems to have been dextral transpression.

North-trending normal faults and grabens in the Ishikari-Yubari Basin indicate that the middle Miocene extensional stress regime documented in southwest Hokkaido also prevailed in central Hokkaido. The largest of these normal faults, the Biratori Fault, is slightly anomalous in that it strikes northwest, suggesting an influence of dextral shear (Sylvester, 1988) or perhaps counterclockwise rotation of the fault during subsequent east-west contraction. Isopachs of the Kawabata Formation (400, 600, and 800 m) connecting between the Yufutsu and Umaoi Faults show a northeast trend of subsidence, but the overall trend of subsidence is northerly because these contours follow a northwest-trend along en echelon, right-stepping normal faults (Figure 14). This "zig-zag" configuration suggests that east-west extension was accompanied by a component of dextral shear. Hence, the stress regime of the Yubari Basin may be best described as dextral transtension. This interpretation is consistent with the northeast-trend of $\sigma_{Hmax} = \sigma_1$ in eastern Hokkaido, and may help to explain the clockwise paleomagnetic rotation of Oligocene to middle Miocene rocks in the Ishikari-Teshiro Belt (Kodama et al., 1993). Hence, the middle Miocene stress field of Hokkaido seems to have been partitioned between east-west extension with a small component of dextral shear in western Hokkaido and dextral transpression on discrete strike-slip faults in eastern Hokkaido.

West Sakhalin Trough

Seismic-reflection records image the West Sakhalin Trough as a 60-km-wide, 450-km-long basin containing an 8-km-thick section of Cenozoic sediment (Antipov et al, 1980; Figure 18), most of which is thought to be

Neogene (Fournier et al., 1994). This narrow sedimentary trough, lying on the east side of Tartar Strait, is bounded on the west by a subcropping ridge of Cretaceous basement and on the east by the West Sakhalin Fault, which connects with the Horonobe Fault in northern Hokkaido (Antipov et al, 1980; Kimura et al., 1983; Lallemand and Jolivet, 1986; Fournier et al., 1994). Antipov et al. (1980) describes narrow, N-trending sub-basins and growth faults within the West Sakhalin Trough consistent with the formation of syndepositional grabens (see Figure 18). Seismic-refraction data indicate that the sedimentary cover in Tartar Strait is underlain by thinned continental crust 18-25 km thick, whereas in Sakhalin and Sikhote-Alin, the crust is 30-38 km thick (Antipov et al., 1980; Gnibidenko and Svarchevsky, 1984). Thinning of the crust is due primarily to elevation of the Moho discontinuity directly beneath Tartar Strait, and is a crustal feature common to rift zones.

Miocene Volcanic Belt

An anomalous, north-trending corridor of Miocene volcanic rocks crops out on both coasts of Tartar Strait and in central Hokkaido (Figure 18). On the Sikhote-Alin coast, the volcanic sequence consists of basalt flows up to 1 km thick interbedded with lacustrine sediment (Antipov et al., 1980; Zonenshain et al., 1990), a sequence typical of continental rifts, where crustal subsidence generates shallow lake basins. In west Sakhalin and the Ishikari-Teshiro Belt, Miocene volcanics occur mainly as dikes and sills of basalt and breccia intruded into upper Oligocene to middle Miocene marine sediment (Nagao et al., 1959; Hoyanagi et al., 1986; Jolivet et al., 1990; Zonenshain et al., 1990; Fournier et al., 1994). Most of the sills and dikes are found in or near fault

zones, which may have served as magma conduits, including the West Sakhalin, Tym-Poronaysk, Yufutsu, and Umaoi Faults.

These volcanics are interpreted to reflect volcanism associated with the crustal rifting and thinning of the continental crust in Tartar Strait and the Ishikari-Teshiro Belt. Some geologists have presumed that the volcanic belt is a volcanic arc associated with subduction of oceanic crust in the Okhotsk Sea beneath Sakhalin (Kimura and Tamaki, 1986; Zonenshain et al., 1990). However, a dense network of seismic-reflection records shows that Neogene strata in the southern Okhotsk Sea are relatively undeformed and do not support the existence of an accretionary-wedge complex offshore (Gnibidenko and Svarchevsky, 1984). It is worth noting that no Miocene volcanism is reported along the southern coast of Sakhalin (Zonenshain et al., 1990), which rifted in the early stages of the opening of the Sea of Japan.

Subsidence of the Sea of Japan

An abrupt change in the middle Miocene benthic foraminiferal fauna from diversified, warm-water species to low-diversity, agglutinated cold-water species is widely recognized along the eastern coast of the Sea of Japan (Tai, 1963, 1985, 1988; Pisciotto et al., 1992). This change, termed the Foram Sharp Line (FSL) by Tai (1963, 1985, 1988), marks the time at which calcareous benthic faunas died off and were replaced by noncalcareous faunas or barren intervals due to rapid subsidence of the basin floor below the calcium carbonate compensation depth. This event is attributed to the late stages of opening of the Sea of Japan (Pisciotto et al., 1992; Tamaki et al., 1992).

In Ocean Drilling Program (ODP) drillholes 794 and 797, the age of the FSL event is estimated at 14.3 Ma, based on planktonic foraminiferal zonation, sedimentation rates, and ^{40}Ar-^{39}Ar dates of drillcore volcanics, and is about the same age as in the onshore sections of northeast Japan (Pisciotto et al., 1992). In ODP drillhole 795, the FSL is 3 m.y. younger at 11.2 Ma, suggesting that the Japan Basin experienced rapid subsidence a few million years later than the Yamato Basin. The FSL event in the Yamato Basin corresponds closely with the end of rifting, graben formation, and thick sedimentation along the west coast of northeast Japan between 18-15 Ma (Yamaji, 1990) and is cited as evidence that these events are directly related (Tamaki et al., 1992; Pisciotto et al., 1992; Fournier et al., 1994). This early Miocene rift zone extends from the Noto Peninsula to north of Okushiri Island and is inferred to include strike-slip faults analogous to the Tanakura Tectonic Line (Lallemand and Jolivet, 1986; Fournier et al., 1994; Figure 18). Similarly, the FSL event in drillhole 795 corresponds closely with the end of graben formation and deposition of thick turbidites in the Ishikari-Teshiro Belt between 14-11 Ma. Hence, east-west extension and crustal rifting in the middle Miocene provides a mechanism to explain rapid subsidence of the Japan Basin at 11.2 Ma, indicated by the age of the FSL in drillhole 795.

Summary

The narrow, 1000-km-long Cenozoic basin consisting of the West Sakhalin Trough and the Ishikari-Teshiro Belt exhibits many features characteristic of crustal rift zones including: (1) an elevated Moho discontinuity, (2) thinned mid-crustal layers, (3) normal faulting and graben

formation, (4) deposition of thick synrift clastic sediment, and (5) association with a belt of extrusive volcanics. The timing of graben formation in southern Hokkaido (14-11 Ma) corresponds closely with rapid subsidence of the Japan Basin inferred from benthic foraminiferal fauna changes in ODP cores. Rapid subsidence of the Yamato Basin was accompanied by rifting and thick deposition on the western margin of the northeast Japan arc. The proposed rift zone along the western margin of Sakhalin and central Hokkaido exhibits an identical pattern of synchronous subsidence, crustal extension, graben formation, and thick deposition of middle Miocene volcaniclastic sediment.

CONCLUSION

The Yubari Fold and Thrust Belt is a zone of late Cenozoic intracontinental convergence that lies between the Kuril and northeast Japan volcanic arcs. Westward-vergent reverse faults and folds deforming a 5-km-thick section of late Cenozoic marine strata record 7 km (25%) of east-west shortening. Growth strata indicate that compressional deformation began between 9 and 4.5 Ma yielding a 0.8 to 1.6 mm/yr estimate for the long-term-average rate of shortening. The primary active structure is a young, blind strand of the Umaoi reverse fault that upwarps shallow seismic reflectors in Quaternary sediment by about 100 m directly above the fault tip. Vertical separation of tidal-flat sediment containing the Toya Ash on either side of the upwarp indicates that the reverse-slip rate of the fault is 0.41±0.04 mm/yr, accounting for 0.26±0.03 mm/yr of east-west convergence. An arched gravel fan, forming a fault-propagation fold in the hanging wall, corroborates late Quaternary slip on the fault. A dated tephra sequence providing a 110±10 ka minimum age for the fan indicates that the rate of uplift of the Northern Umaoi Hills Arch is greater than 0.66±0.17 mm/year.

Post-late Miocene convergence was preceded by middle Miocene extension and normal faulting. The reverse faults of the Yubari Fold and Thrust Belt are reactivated middle Miocene normal faults that controlled deposition of the Kawabata Formation between 14 and 11 Ma and define the western margin of a graben. This graben is part of an unrecognized, 1000-km-long and 60-km-wide, failed crustal rift that includes the West Sakhalin Trough in the Russian Far East and the Ishikari-Teshiro Belt in Hokkaido. The rift is expressed as a linear basin that exhibits many features characteristic

of crustal rifting including: (1) an elevated Moho discontinuity, (2) thinned mid-crustal layers, (3) bounding normal faults and grabens, 4) thick synrift clastic sediments, and (5) association with a belt of extrusive volcanics. The timing of graben formation (14-11 Ma) in southern Hokkaido corresponds closely with rapid subsidence of the adjacent Sea of Japan basin inferred from benthic foraminifer data in ODP cores. Hence, middle Miocene east-west extension along the eastern margin of the Sea of Japan seems to have played an important role in the final stages of opening of the Sea of Japan. Further studies are needed to test the rift model and to evaluate the role of east-west extension in the opening of the Sea of Japan.

BIBLIOGRAPHY

Agatsuma, M., 1961, On the subsurface structures of the Yuni plain and Umaoi hill: Journal of the Japanese Association of Petroleum Technologists, v. 26, p. 169-179, 339-345 (in Japanese).

Agatsuma, M., 1962, A study on the subsurface structure of the Ishikari depression in central Hokkaido: Journal of the Japanese Association of Petroleum Technologists, v. 27, p. 345-382 (in Japanese).

Anstey, N.A., 1977, Seismic Interpretation: The Physical Aspects: International Human Resources Development Corporation, Boston.

Antipov, M.P., Kovylin, V.M., and Filat'yev, V.P., 1980, Sedimentary cover of the deepwater basin of Tartar Strait and the northern part of the Japan Sea: International Geology Review, v. 22, p. 1327-1334.

Arai, F., Machida, H., Okumura, K., Miyauchi, T., Soda, T., and Yamagata, K., 1986, Catalog for late Quaternary marker-tephras in Japan II - Tephras occurring in northeast Honshu and Hokkaido: Geographical Report of Tokyo Metropolitan University, no. 21, p. 223-250.

Asano, S., Den, N., Hotta, H., Yoshii, T., Ichinose, Y., Sakajiri, N., and Sasatani, T., 1979, Seismic refraction and reflection measurements around Hokkaido, Part 2. Crustal structure of the continental slope off Hidaka: Journal of Physics of the Earth, v. 27, p. 497-509.

Asano, S., Takahashi, A., and Ikawa, T., 1985, Study on the deep geological structure of Ishikari, Hokkaido, for precise estimation of local earthquake ground motion, chapter 4: Special report on natural hazards to the Ministry of Education, project No. A-63-3 (in Japanese with English abstract).

Blow, W.H., 1969, Late middle Eocene to recent planktonic foraminiferal biostratigraphy: *in* Bronnimann, P., and Renz, H. eds., proceedings of the First International Conference on Planktonic Microfossils, v. 1, p. 119-421.

Boothroyd, J.C., and Nummedal, D., 1978, Proglacial braided outwash: a model for humid alluvial-fan deposits, *in* Miall, A. ed., Fluvial Sedimentology: Calgary, Canadian Society of Petroleum Geologists, p. 641-668.

Boyer, S.E., 1986b, Styles of folding within thrust sheets: examples from the Appalachian and Rocky Mountains of the U.S.A. and Canada: Journal of Structural Geology, v. 8, p. 325-340.

Chapman, M.E., and Solomon, S.C., 1976, North American-Eurasian plate boundary in northeast Asia: Journal of Geophysical Research, v. 81, p. 921-930.

Chinzei, K., 1986, Opening of the Japan Sea and marine biogeography during the Miocene: Journal of Geomagnetism and Geoelectricity, v. 38, p. 487-494.

Commission for the Promotion of Mining in Hokkaido, 1968, Exploration and development of oil and gas resources in Hokkaido: special study commissioned by the Hokkaido Prefectural Office, March 1968, 183 p. (in Japanese).

Commission for the Promotion of Mining in Hokkaido, 1990, Exploration and development of oil and gas resources in Hokkaido: special study commissioned by the Hokkaido Prefectural Office, March 1990, 157 p. (in Japanese).

DeMets, C., Gordon, R.G., Argus, D.F., and Stein, S., 1990, Current plate motions: Geophysical Journal International, v. 101, p. 425-478.

Den, N., and Hotta, H., 1973, Seismic refraction and reflection evidence supporting plate tectonics in Hokkaido: Papers in Meteorology and Geophysics, v. 24, p. 31-54.

Fournier, M., Jolivet, L., Huchon, P., Sergeyev, K.F., and Oscorbin, L. S., 1994, Neogene strike-slip faulting in Sakhalin and the Japan Sea opening: Journal of Geophysical Research, v. 99, p. 2701-2725.

Geographical Survey Institute of Japan, 1974, Aerial photographs, series HO-74-9Y - C9B-5 to 10, - C12B-7 to 11, - C11B-7 to11, - C6-10 to 13, - C5-9 to13, - C8B-14 to 18, - C10B-5 to 11, scale 1:40,000, black-and-white.

Geological Survey of Japan, 1992, Geological map of Japan, 3rd. edition, scale 1:1,000,000.

Gnibidenko, H.S., and Svarichevsky, A.S., 1984, Tectonics of the south Okhotsk deep-sea basin: Tectonophysics, v. 102, p. 225-244.

Hilgen, F.J., 1991, Astronomical calibration of Gauss to Matuyama sapropels in the Mediterranean and implication for the geomagnetic polarity time scale: Earth and Planetary Science Letters, v. 104, p. 226-244.

Holt, W.E., and Stern, T.A., 1994, Subduction, platform subsidence and foreland thrust loading: the late Tertiary development of Taranaki Basin, New Zealand: Tectonics, v. 13, p. 1068-1092.

Hoyanagi, K., Miyasaka, S., Watanabe, Y., Kimura, G., and Matsui, M., 1986: Deposition of turbidites in the Miocene collision zone, central Hokkaido, *in* Geology and Tectonics of Hokkaido: Association for the Geological Collaboration in Japan, Monograph no. 31, p. 265-284 (in Japanese with English abstract).

Ishida, M., Soya, T., and Suda, Y., 1980, Geologic map, Sapporo area, 1:200,000 series, Sapporo sheet NK-54-14, Geological Survey of Japan (in Japanese with English explanation).

Ishizuka, H., 1981, Greenstones from the Idonnappu formation along the river Oku-Niikappu in axial zone of Hokkaido, Japan: Memoirs of the Faculty of Science, Kochi University, v. 2, p. 1-22.

Jolivet, L., and Huchon, P., 1989, Crustal-scale strike-slip deformation in Hokkaido, northern Japan: Journal of Structural Geology, v. 11, p. 509-522.

Katsui, Y., 1959, On the Shikotsu pumice fall deposit: Bulletin of the Volcanological Society of Japan, v. 4, p. 33-48 (in Japanese).

Kiminami, K., and Kontani, Y., 1983, Mesozoic arc-trench systems in Hokkaido,*in* Hashimoto, M., and Uyeda, S., eds., Accretion tectonics in the circum-Pacific regions, proceedings Oji international seminar on accretion tectonics, September 1981: Tokyo, Terra Scientific Publishing Co., p. 107-122.

Kimura, G., 1981, Tectonic evolution and stress field in the southwestern margin of the Kurile Arc: Journal of the Geological Society of Japan, v. 87, p. 757-768 (in Japanese with English abstract).

Kimura, G., 1986, Oblique subduction and collision: Forearc tectonics of the Kuril arc: Geology, v. 14, p. 404-407.

Kimura, G., Miyashita, S., and Miyasaka, S., 1983, Collision tectonics in Hokkaido and Sakhalin, *in* Hashimoto, M., and Uyeda, S., eds., Accretion tectonics in the circum-Pacific regions, proceedings Oji international seminar on accretion tectonics, September 1981: Tokyo, Terra Scientific Publishing Co., p. 123-134.

Kimura, G., and Tamaki, K., 1986, Collision, rotation, and back-arc spreading: the case of the Okhotsk and Japan Seas: Tectonics, v. 5., p. 389-401.

Komada, K., Takeuchi, T., and Ozawa, T., 1993, Clockwise tectonic rotation of Tertiary sedimentary basins in central Hokkaido, northern Japan: Geology, v. 21, p. 431-434.

Kondo, T., Igarashi, Y., Yoshida, M., and Akamatsu, M., 1984, Quaternary deposits in the borehole at Shizukawa, Tomakomai City, Hokkaido, Japan: The Quaternary Research, v. 22, p. 313-325.

Lallemand, S., and Jolivet, L., 1986, Japan Sea: a pull-apart basin: Earth and Planetary Science Letters., v. 76, p. 375-389.

Lillie, R.J., Johnson, G.D., Yousaf, M., Zaman, A., and Yeats, R.S., 1987, Structural development within the Himalayan foreland fold and thrust belt of Pakistan: Canadian Society of Petroleum Geologists, Memoir No. 12, p. 379-392.

Lindseth, R.O., 1968, Digital processing of geophysical data: Society of Exploration Geophysics, Cont. Educ. Prog., p. L1-L4.

Ludwig, W., 1966, Sediments and structure of the Japan Trench: Journal of Geophysical Research, v. 71, p. 2121-2137.

Machida, H., Arai, F., and Momose, M., 1985, Aso-4 ash: A widespread tephra and its implications to the events of the late Pleistocene in and around Japan: Bulletin of the Volcanological Society of Japan, v. 30, p. 49-70 (in Japanese with English abstract).

Machida, H., Arai, F., Miyauchi, T., and Okumura, K., 1987, Toya ash - A widespread late Quaternary time-marker in northern Japan: The Quaternary Research, v. 26, p. 227-242.

Machida, H., 1991, Recent progress in tephra studies in Japan: The Quaternary Research, v. 30, p. 141-149.

Maiya, S., Ichinoseki, T. and Akiba, F., 1981, Stratigraphic outlines of selected Neogene sequences - Hidaka area, in Tsuchi, R., ed., Neogene of Japan-Its Biostratigraphy and Chronology, IGCP-114 national working group of Japan, p. 85-89.

Matsuno, K., and Ishida, M., 1960, Geologic map and explanatory text, Hayakita sheet, 1:50, 000 scale, Geological Survey of Japan, Hokkaido Development Agency, 35 p. (in Japanese with English abstract and explanation).

Matsuno, K., and Hata, M., 1960, Geologic map and explanatory text, Oiwake sheet, 1:50,000 scale: Geological Survey of Japan, Hokkaido Development Agency 34 p. (in Japanese with English abstract and explanation).

McCaffrey, R., Estimates of modern arc-parallel strain rates in fore arcs: Geology, *in press*, November 1985.

Mitani, K., 1978, Changing of the Tertiary sedimentary basins in the western flank of axial belt of Hokkaido - bearing a significance of the Sunagawa Lowland to Umaoi hilly belt: Association for Geological Collaboration in Japan, Monograph no. 21, p. 127-137 (in Japanese).

Miyamachi, H. and Moriya, T., 1984, Velocity structure beneath the Hidaka mountains in Hokkaido, Japan: Journal of Physics of the Earth, v. 32, p. 13-42.

Moore, G.W., Drummond, K.J., Uyeda, S., Bogdanov, N.A., Simkin, T., Siebert, L., Golovchenko, X., Larson, R.L., Pitman III, W.C., Rinehart, W.A., 1992, Plate-tectonic map of the circum-Pacific region, Arctic sheet: U.S. Geological Survey Circum-Pacific Map Series CP-41, scale 1:10,000,000.

Murauchi, S., and Ludwig, W., 1980, Crustal structure of the Japan Trench: the effect of subduction of the ocean crust: Initial Reports of the Deep Sea Drilling Project, Legs 56 and 57, Part 1, U.S. Government Printing Office, p. 463-469.

Nagao, S., Osanai, H., and Ishiyama, S., 1959, Geologic map, Eniwa sheet, 1:50,000 scale: Geological Survey of Japan, Hokkaido Development Agency (in Japanese with English and explanation).

Nakamura, K., 1983, Possible nascent trench along the eastern Japan Sea as the convergent boundary between Eurasian and North American plates: Bulletin of the Earthquake Research Institute, v. 58, p. 711-722 (in Japanese with English abstract).

Nakamura, K. and Uyeda, S., 1980, Stress gradient in arc-back arc regions and plate subduction: Journal of Geophysical Research, v. 85, p. 6419-6428.

Niitsuma, N., Konishi, K., Wada, H., Kitazato, H., Amano, K., and Minoura, K., 1982, Pre-existing boring data: summary report, Mombusho Grant-in-Aid No. 56306013, 137 p.

Normark, W.R., Posamentier, H., and Mutti, E., 1993, Turbidite systems; state of the art and future directions: Reviews of Geophysics, v. 31, p. 91-116.

Okada, H., 1978, Sedimentary patterns in apparent back-arc basins: a case study of the Neogene sequence in northwestern Hokkaido, Japan, *in* Uyeda, S., Murphy, R., and Kobayashi, K., eds., Geodynamics of the western Pacific: Journal of Physics of the Earth, v. 26, supplement, p. 477-490

Okada, H., 1983, Collision orogenesis and sedimentation in Hokkaido, Japan, *in* Hashimoto, M., and Uyeda, S., eds., Accretion tectonics in the circum-Pacific regions, proceedings Oji international seminar on accretion tectonics, September 1981: Tokyo, Terra Scientific Publishing Co., p. 91-105.

Okamura, S., Katoh, T., Shibata, K., Ganzawa, Y., and Uchiumi, S., 1992, Cretaceous granitoids from the well at the eastern area of Tomakomai, Hokkaido: Journal of the Geological Society of Japan, v. 98, p. 547-550 (in Japanese).

Okumura, K., 1987, Quaternary crustal movements of Hokkaido, north Japan, estimated from deformed marine terraces: Ph. D dissertation, Dept. of Geography, Faculty of Science, University of Tokyo, 247 p. (in Japanese with English abstract).

Okumura, K., 1988, Recurrence of large pyroclastic flows and innovation of volcanic activity in eastern Hokkaido, Japan: Proceedings Kagoshima International Conference on volcanoes, p. 518-521.

Okumura, K., 1991, Quaternary tephra studies in the Hokkaido District, northern Japan: The Quaternary Research, v. 30, p. 379-390.

Ono, K., Matsumoto, Y., Miyahisa, M., Teraoka, Y., and Kambe, N., 1977, Geology of the Taketa district: Geological Survey of Japan, 56 p.

Pisciotto, K.A., Ingle, J.C., Jr., von Breymann, M.T., Barron, J., and Nomura, R., 1992, Miocene benthic foraminifers at sites 794, 795, and 797 in the Sea of Japan with reference to the foram sharp line in the Honshu arc: Proceedings of the Ocean Drilling Program, Scientific Results, v. 127/128, p. 493-540.

Ponti, D., Barron, J.A., Sarna-Wojcicki, A.M., Cotton, M.L., Hummon, C., and Schneider, C.L., 1993, Benthic foram biostratigraphy and the age of the Pico Formation in the northern Los Angeles basin: potential problems for evaluating activity of blind thrust faults: Transactions, American Geophysical Union, fall meeting supplement, p. 434.

Research Group for Active Faults of Japan, 1991, Active faults in Japan: sheet maps and inventories, University of Tokyo Press, second edition, 437 p.

Sangawa, A., Kinugasa, Y., and Kakimi, T., 1986, A new series of the Neotectonic maps of Japan, Sapporo sheet 4, 1:500,000 scale: Bulletin of the Geological Society of Japan, v. 34, p. 27-37 (in Japanese with English abstract and explanation).

Sasa, Y., Tanaka, K., and Hata, M., 1964, Geologic map and explanatory text, Yubari sheet, 1:50, 000 scale: Geological Survey of Japan, Hokkaido Development Agency, 184 p. (in Japanese with English abstract and explanation).

Seno, T., 1985a, Is northern Honshu a microplate?: Tectonophysics, v. 115, p. 177-196.

Sherrif, 1978, Geophysical Exploration and Interpretation: Boston, International Human Resources Development Corporation, 313 p.

Shibata, K., Uchiumi, S., Uto, K., and Nakagawa, T., 1984, K-Ar results, Part 2, new data from the Geological Survey of Japan: Bulletin Geological Survey of Japan, v. 35, p. 331-340.

Sugi, N., Chinzei, K., and Uyeda, S., 1983, Vertical crustal movements of northeast Japan since middle Miocene, *in* Hilde, T., and Uyeda, S., eds., Geodynamics of the Western-Pacific-Indonesian Region: American Geophysical Union Geodynamics Series, v. 11, p. 317-329.

Suppe, J., 1985, Principles of structural geology: Englewood Cliffs, N.J., Prentice-Hall, Inc., 537 p.

Suppe, J., and Medwedeff, D.A., 1990, Geometry and kinematics of fault-propagation folding: Eclogae Geol. Helv., v. 83, p. 409-454.

Sylvester, A.G., 1988, Strike-slip faults: Geological Society of America Bulletin, v. 100, p. 1666-1703.

Tai, Y., 1963, Historical change in the Neogene foraminiferal assemblages in the Stouchi and San-in provinces and Foram Sharp Line: Kaseki (Fossils), v. 5, p. 1-7 (in Japanese).

Tai, Y., 1985, On so-called Foram Sharp Line: Hiroshima University, Faculty of Integrated Arts and Science, Memoir IV, v. 10, p. 17-33 (in Japanese).

Tai, Y., 1988, Foraminiferal Sharp Line and its microbiostratigraphic significance: Mukugawa Women's University, Education Bulletin, v. 35, p. 87-103.

Tamaki, K., Suyehiro, K., Allan, J., Ingle, J.C., and Pisciotto, K.A., 1992, Tectonic synthesis and implications of Japan Sea ODP drilling: Proceedings of the Ocean Drilling Program, Scientific Results, v. 127/128, p. 1333-1348.

Tsuchida, S., 1961, Geological structure of the Neogene formations in the middle part of Ishikari plane (Sapporo Lowland) in Hokkaido, Japan: Journal of the Japanese Association of Petroleum Technologists, v. 26, p. 20-28, 51-56, 180-187 (in Japanese).

Umaoi-Collaborative Research Group, 1987, Late Pleistocene stratigraphy and paleogeography of the eastern marginal area of the Ishikari Lowland, central Hokkaido, Japan: Earth Science, v. 41, p. 303-319 (in Japanese-translated into English by K. Kimura, Geological Survey of Japan).

von Huene, R., Langseth, M., Nasu, N., and Okada, H., 1982, A summary of Cenozoic tectonic history along the IPOD Japan Trench transect: Geological Society of America Bulletin, v. 93, p. 829-846.

Watanabe, Y., and Iwata, K., 1985, The age of the Miocene Kamishiyubetsu Formation in northern Hokkaido and the basins formed by tectonic movement: Journal of the Geological Society of Japan, v. 91, p. 427-430.

Woodward, N.B., Boyer, S.E., and Suppe, J., 1989, Balanced geological cross sections: an essential technique in geological research and exploration: American Geophysical Union, Short Course in Geology Series, v. 6, , 132 p.

Zonenshain, L.P., Kuzmin, M.I., and Natapov, L.M., 1990, Sikhote-Alin-Sakhalin foldbelt, *in* Page, B., ed., Geology of the USSR: a plate tectonic synthesis: American Geophysical Union Geodynamics Series v. 21, p. 109-120.

APPENDICES

APPENDIX 1

Analysis of Seismic-Reflection Data

Key seismic reflectors in records Yuni-Shuhen V6 and V7 were converted from time display to depth display using a time-depth conversion chart (Figure A1.1). This chart was modified from the depth-conversion chart of Asano et al. (1985) for record Naganuma 85, and represents an estimated average of the seismic velocities along the Yuni-Shuhen V6 and V7 seismic lines. The chart of Asano et al. (1985) is based on data from the Ishikari Lowland, where thicker, low-velocity sediment overlies the Neogene section. Hence, the principal modification was to increase the seismic velocity of the near-surface materials in the first 1 second of two-way travel time. The following section describes the data and methodology used to refine the chart of Asano et al. (1985).

Determination of Seismic Velocity

Empirical relationships show that the seismic velocity of any given substrate is exponentially proportional to its density (Anstey, 1977). Variation in density is due primarily to porosity (including tectonically-induced microfracturing) and the filling of pore spaces by water. Agatsuma (1961) reported average specific gravities (g/cm^3) for the Biratori Formation (1.66), the Kawabata Formation (1.96), and Takinoue Formation, based on 62 rock samples collected in the Umaoi Hills. Applying these values to the empirical curves yields seismic velocity estimates ranging between 2,210-2,940 m/s. Because these samples reflect substrate densities in the surficial weathering zone (a zone generally characterized by reduced seismic velocity), these

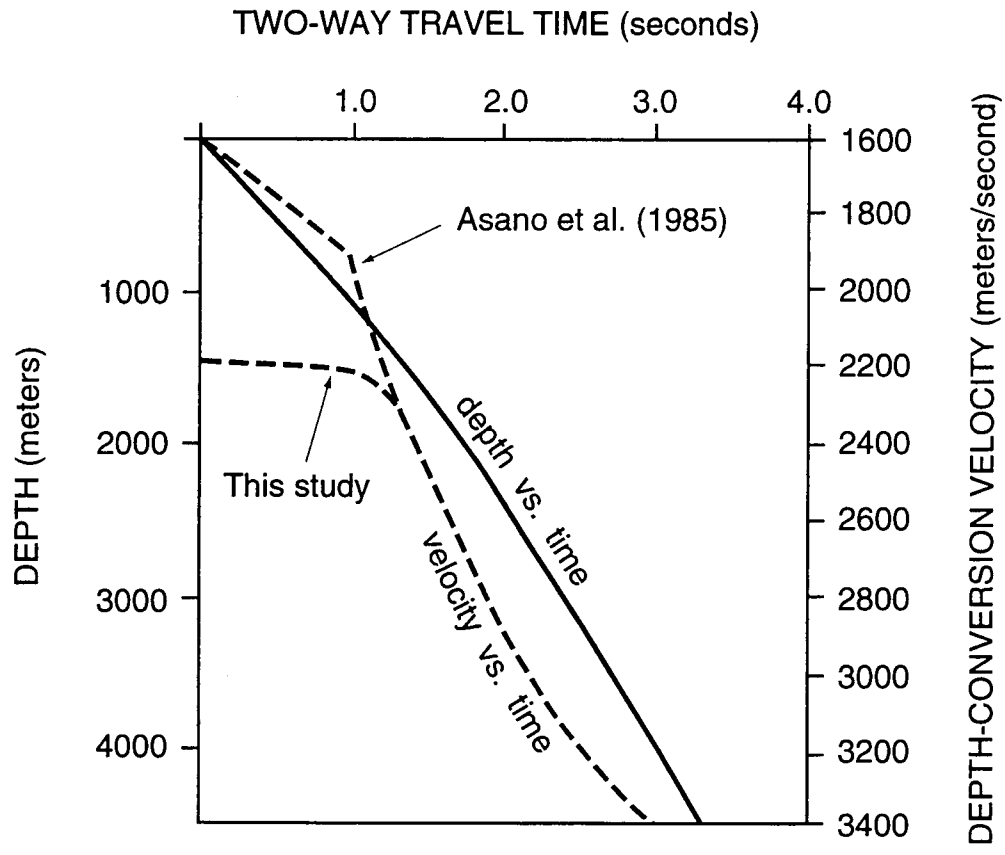

Figure A1.1 Chart showing the relationships between two-way travel time, substrate depth, and velocity that were used to convert seismic-reflection records Yuni-Shuhen V6 and V7 from time sections to depth sections. Sharp increase in velocity gradient at about 1 second marks average boundary between unconsolidated sediment and weathered rock zone in the near surface and underlying bedrock.

estimates are probably less than the seismic velocities below the weathering zone. During a railway-tunneling project in the southern Umaoi Hills, near-surface seismic velocities of the Karumai and Biratori Formations were measured at 1,800-2,700 m/s (unpublished data, Japan Railways, date unknown).

In general, these measurements and empirical estimates compare well with the interval stacking velocities of Asano et al. (1985) which range from 1,600-3,650 **m/s** for substrate in the first 4.0 seconds of two-way travel time. However, because low-velocity sediment is much thinner around the Umaoi Hills than in the Ishikari Lowland, the seismic velocity of the near surface materials along seismic lines Yuni-Shuhen V6 and V7 is greater than that used by Asano et al. (1985). In addition, measured seismic velocities of near - surface sediments at the western foot of the Umaoi Hills (1,710-2,170 m/s) (unpublished data, Geological Survey of Japan, 1992) are greater than in the Ishikari Lowland. The stacking velocity used by Asano et al. (1985) for the interval of 0.0 to 1.0 seconds of two-way travel time was 1,750 m/s. Because this value is less than the average of the measured and empirical values at the Umaoi Hills, the depth conversion chart of Asano et al. (1985) was modified such that the average velocity in the 0.0 to 1.0 second interval is 2,200 m/s.

APPENDIX 2

Tephra Analysis Data

The following table shows the major-element chemistry of tephra samples identified in Figure 5 as determined by induced coupled plasma (ICP) analysis. This analysis was performed by the Geological Survey of Japan in 1991. Values are reported in weight %, and sampling locations are shown in figure 15.

Sam-ple	Tephra Name	TiO2	Al2O3	Fe2O3	MgO	MnO	CaO	K2O	Na2O	P2O5
B1*	Toya	0.05 ±0.01	11.79 ±0.24	0.85 ±0.05	0.04 ±0.01	0.09 ±0.02	0.35 ±0.03	2.29 ±0.13	4.07 ±0.38	
C1	Mpfa-3	0.37	13.41	2.48	0.33	0.07	2.52	1.7	3.08	0.05
E1	Spfa-1	0.12	12.59	2.05	0.15	0.06	2.12	1.74	3.05	0.03
E2	Spfa-10	0.36	14.12	2.36	0.34	0.06	3.45	1.99	3.37	0.10
E3	Aso-4	0.45	14.27	1.9	0.35	0.11	1.51	3.81	4.45	0.08
E4	Toya	0.06	11.04	1.17	0.02	0.10	0.43	2.38	4.32	0.02
E5	Kc-Hb	0.35	11.71	2.18	0.29	0.06	1.86	2.11	3.38	0.05
F1	Toya	0.06	11.72	1.16	0.02	0.10	0.52	2.46	4.59	0.02

Error associated with ICP analysis is 3-5% for values greater than 10 ppm.

* Analysis for sample B taken from Okumura (1987). Value reported in Fe_2O_3 column was measured as FeO.

Figure A2.1 shows the refractive index of glass-shard samples measured at the Seismotectonics Section of the Geological Survey of Japan by K.

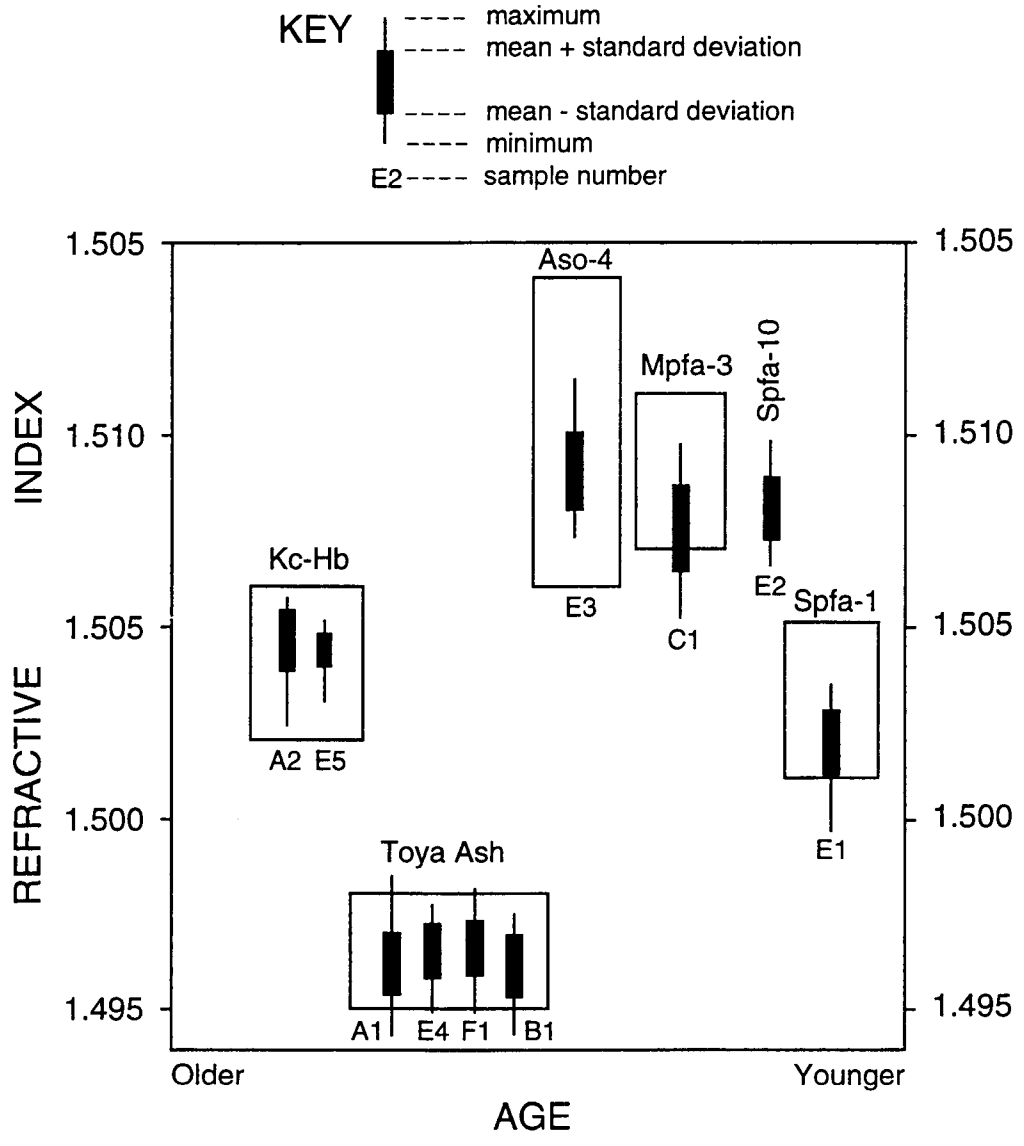

Figure A2.1 Refractive index values of glass shards from sampled tephras. These data were used, in conjunction with major-element chemistry, to identify and correlate tephras. Sample locations are shown in figures 5 and 15. Open boxes show known range in refractive index after Arai et al. (1986), Machida et al. (1987), and Machida (1991).

Shimokawa. The index of refraction n is a measure of the speed of light waves through a medium v in relation to the speed the light through air c, as given by the formula $n=c/v$. These measurements were made with the R1MS87 Refractive Index Measuring System instrument, manufactured by the Kyoto Fission-Track Company, Ltd., Kyoto, Japan. The basic methodology is to immerse the sample in oils of various refractive indexes and measure the refraction of light as it travels between the two mediums. When a sample is immersed in an oil with an identical refractive index, light is not refracted as it travels from one medium to the other.

Tephra identifications in drillcore E are based on major-element chemistry and refractive index. Tephras in drillcore A are identified from refractive index correlation with drillcore E. These data support previous correlations of the Aafa-2 tephra with the Toya ash (Arai et al., 1986) and tentative correlation of the Aafa-3 tephra with the Kc-Hb tephra (personal communication, K. Shimokawa, 1992).

APPENDIX 3

Error Analysis for Rates of Tectonic Activity

Western strand of the Umaoi Fault

The amount of late Quaternary reverse slip on the western strand of the northern segment of the Umaoi Fault was calculated using the vertical displacement of the Toya Ash across the fault (29.5 meters) and the dip of the fault plane (50°). Using the sine law, the amount of reverse slip is the hypotenuse of a right triangle with the side opposite a 50° angle being 29.5 meters long.

$$s = 29.5 \text{ m} / \sin 50° = 38.5 \text{ m}$$

The altitude of the Toya Ash is estimated from 1:25,000 scale topographic maps with a primary contour interval of 10 m and supplemental interval of 5 m. From these maps, the altitude of a particular location may be estimated within 3 meters of the true elevation. Hence, the error associated with an altitude read from the map is estimated to be ±1.5 meters. The altitude of the Toya Ash in drillhole A was tied to the vertical datum of the 1:25, 000 topographic map with a survey instrument, and therefore, contributes negligible error. This translates into a range in the reverse slip estimate of 36.5 to 40.5 meters as shown by the following calculations.

$$s = (29.5\ m - 1.5\ m) / \sin 50° = 36.5\ m$$

$$s = (29.5\ m + 1.5\ m) / \sin 50° = 40.5\ m$$

The reported error associated with the age of the Toya ash is ±5,000 years (Machida et al., 1987). Combining these two sources of error yields an error estimate for the reverse slip rate of the fault of ±0.04 mm/year. Similarly, the error associated with the convergence rate of the fault is ±0.03.

Northern Umaoi Hills

The uplift estimate for the Northern Umaoi Hills Arch was calculated by comparing the elevation of the constructional surface at the crest of the uplift to the estimated depositional geometry of the Abira Formation gravel fan. An empirical relationship between clast size and fan slope indicates that the original depositional slope was 6±2 m/km (Boothroyd and Nummedal, 1978). This range in slope is further constrained by gravel exposures that limit the permissible range in the constructional slope to between 4 m/km and 6.9 m/km. Comparison of the range in possible undeformed geometries with the deformed geometry shown in Figure 7 indicates uplift at the crest of the arched gravel of 60 to 82 m. As discussed previously, measurement error associated with altitudes read from 1:25,000 scale topographic maps is estimated to be ±1.5 m. The addition of these two sources of error result in an uplift and error estimate of 71±12.5 m.

The reported error associated with age of the Kc-Hb tephra is ±10,000 years (Machida, 1991). Combining the above sources of error yields an estimate for the uplift of the northern Umaoi Hills of 0.66±0.17 mm/year, as shown in the following calculation.

Uplift rate = 71±12.5 m / 110,000±10,000 years
= 0.83 (maximum) to 0.49 (minimum) mm/year
= 0.66±0.17mm/year